Vol. 84 (1993) *ACTA PHYSICA POLONICA A* No. 1

Proceedings of the VI International School on Magnetism, Białowieża '92

MAGNETIC FORM FACTOR MEASUREMENTS BY POLARISED NEUTRON SCATTERING: APPLICATION TO HEAVY FERMION SUPERCONDUCTORS

K.-U. NEUMANN AND K.R.A. ZIEBECK

Department of Physics, Loughborough University of Technology
Loughborough, LE11 3TU, Great Britain

The experimental technique of spin polarised neutron scattering as used in magnetic form factor measurements is presented. An introduction to the interpretation and the calculation of magnetic form factors and magnetization densities is given. The experimental technique of neutron scattering theory as applied to elastic spin polarised scattering experiments is briefly introduced. The calculation of the magnetic form factor and the magnetization densities are considered for simple model systems such as a collection of localised magnetic moments or an itinerant electron system. The discussion is illustrated by an experimental investigation of the magnetic form factor in the heavy fermion superconductors UBe_{13} and UPt_3. Magnetization density maps and magnetic form factors are presented, and their implications for other physical quantities are briefly discussed.

PACS numbers: 75.25.+z, 71.28.+d

1. Introduction

Neutron scattering and in particular spin polarised neutron scattering is a powerful tool for the characterization and investigation of physical properties on an atomic scale. The charge neutrality and magnetic dipole moment of the neutron make it an ideal probe for the investigation of magnetic degrees of freedom. In addition to using neutron scattering for investigating phenomena connected with magnetism (by e.g. establishing the nature of magnetically ordered states), experiments may be devised for the characterization of details of electronic wave functions. Such an experiment is realised when spin polarised neutrons are used for the determination of the magnetic form factor and of the magnetization density. Contrary to spectroscopic techniques which infer details of the wave function by an investigation of the experimentally determined level scheme (e.g. the crystal field levels of localised f moments) magnetic form factor measurements referred

to here are elastic measurements and therefore these measurements do not involve an energy transfer between neutron and target. Consequently this method does not yield direct information on the energy eigenvalues of the Hamiltonian, that is the energy levels or band structure of the system under investigation. Instead a magnetic form factor investigation can be classified as an investigation of the real space properties of some electronic wave functions. This point will be discussed more fully below, and a clarification will be given as to what exactly is meant by "some electronic wave functions". The investigation of the magnetic form factor by spin polarised neutron scattering is therefore complementary to experiments such as de Haas–van Alphen measurements, which investigate the details in momentum space of energy levels and the Fermi surface.

In order to be able to fully appreciate the potential of spin polarised neutron scattering for the investigation of magnetization densities and magnetic form factors a brief introduction is given to the experimental technique. First, the basic principles are reviewed of elastic nuclear and magnetic scattering, and a derivation is given for the description of a magnetic form factor measurement. Two simple models, a localised moment system and an itinerant electron model, are considered, and for each of these model systems a magnetic form factor experiment is analysed. In the second section the theory is illustrated using the results of an experimental investigation. A magnetic form factor measurement is considered which was carried out on the heavy fermion compounds UBe_{13} and UPt_3. The experimental magnetization densities and form factors are presented and discussed in relation to the simple model systems mentioned above. Some consequences of the experimental findings are briefly discussed.

2. Magnetic form factor measurements

Magnetic form factor measurements are usually carried out on single crystals employing spin polarised neutrons. The discussion here will be limited to the case of a paramagnetic material with a crystallographic structure which has a centre of inversion symmetry.

An experimental determination of the magnetic form factor comprises of two different measurements. By using unpolarised neutrons, a first experiment establishes the details of the nuclear structure of the crystal under investigation. In a second experiment and by using spin polarised neutrons a quantity known as the flipping ratio is determined for a number of Bragg reflections.

In order to establish the details of the nuclear structure it is important to carry out both experiments on the same single crystal and preferably also at the same temperature. The nuclear structure is determined by measuring the integrated intensity of Bragg reflections. A subsequent refinement of a crystallographic model and its comparison with the measured Bragg intensities is used to establish important parameters such as lattice site occupations and temperature factors. In this way the nuclear structure factor is determined precisely.

In a second experiment the Bragg reflection is measured using spin polarised neutrons and with the crystal in an external magnetic field. Due to the presence of a magnetic field a ferromagnetic moment is induced in the paramagnet. As a result of

the induced ferromagnetic order magnetic Bragg scattering occurs. The magnetic scattering arises in addition to nuclear scattering. As both the magnetic and the nuclear unit cell have the same dimensions, magnetic and nuclear Bragg reflections are superimposed. It turns out that this superposition is more than a mere addition of nuclear and magnetic intensities. By using spin polarised neutrons it is possible to make use of an interference term in the scattering cross-section between nuclear and magnetic scattering. This combination of magnetic and nuclear scattering in the neutron scattering cross-section can be used to precisely determine a quantity known as the flipping ratio. The flipping ratio is a function of the magnetic and nuclear structure factors. If the nuclear structure factor is known, a measurement of the flipping ratio allows a very precise determination of the magnetic structure factor. The physical significance of the entities mentioned here will be discussed more fully below. A more detailed analysis of the theory of neutron scattering can be found in standard text books [1–4].

2.1. Nuclear scattering

For structure determination and for the measurement of the magnetic form factors it suffices to restrict the description of nuclear scattering of neutrons to elastic scattering only. In particular, it is only the integrated Bragg scattered intensity which is of relevance here. By definition the Bragg scattering is elastic scattering with no energy transfer between the crystal and the neutron. The differential neutron scattering cross-section can be written in the form

$$\frac{\mathrm{d}\sigma}{\mathrm{d}\Omega}(\boldsymbol{k}) = \left|\sum_i b_i \mathrm{e}^{\mathrm{i}\boldsymbol{k}\cdot\boldsymbol{R}_i}\right|^2 = \sum_{i,j} b_i b_j \mathrm{e}^{\mathrm{i}\boldsymbol{k}\cdot(\boldsymbol{R}_i-\boldsymbol{R}_j)}, \tag{1}$$

where b_i is the scattering length of the atom i which is located at position $\boldsymbol{R}_i$. $\boldsymbol{k}$ is the neutron scattering vector and $\mathrm{d}\Omega$ is the infinitesimal solid angle into which the neutrons are scattered. The summation is carried out over all atoms in the crystal.

Making use of the translational symmetry of the crystallographic structure, the summation in (1) may be separated into two partial sums

$$\sum_i b_i \mathrm{e}^{\mathrm{i}\boldsymbol{k}\cdot\boldsymbol{R}_i} = \sum_\nu \mathrm{e}^{\mathrm{i}\boldsymbol{k}\cdot\boldsymbol{R}_\nu}\left(\sum_{j(\nu)} \mathrm{e}^{\mathrm{i}\boldsymbol{k}\cdot(\boldsymbol{R}_j-\boldsymbol{R}_\nu)}\right). \tag{2}$$

Here the index ν sums over all unit cells of the crystal and the summation j is carried out over all atoms within the unit cell ν. The position of the atoms in each unit cell is given by $\boldsymbol{R}_j - \boldsymbol{R}_\nu$ and it is measured relative to the origin of the ν-th unit cell as determined by $\boldsymbol{R}_\nu$. A nuclear structure factor of the unit cell $F_N(\boldsymbol{k})$ may be defined as

$$F_N(\boldsymbol{k}) = \sum_i b_i \mathrm{e}^{\mathrm{i}\boldsymbol{k}\cdot\boldsymbol{R}_i}, \tag{3}$$

where the atomic position $\boldsymbol{R}_i$ is measured with respect to the origin of the unit cell. In general, $F_N(\boldsymbol{k})$ will be a complex number. However, for a crystallographic

structure with a centre of inversion symmetry the nuclear structure factor may be chosen to be real. (By taking the point of inversion symmetry as the origin of the unit cell, every atom at position $\boldsymbol{R}_i$ has its symmetry related atom located at $-\boldsymbol{R}_i$ and with the atom having the same scattering length. As a consequence, every contribution $b_i \exp(i\boldsymbol{k} \cdot \boldsymbol{R}_i)$ in (3) is combined with its complex conjugate $b_i \exp(-i\boldsymbol{k} \cdot \boldsymbol{R}_i)$ and in the summation the imaginary parts cancel.)

Inserting (3) into (1) and carrying out the summation over all unit cells one arrives at

$$\frac{d\sigma}{d\Omega}(\boldsymbol{k}) = N \sum_{\tau} |F_N(\boldsymbol{k})|^2 \, \delta(\boldsymbol{k} - \boldsymbol{\tau}). \tag{4}$$

Here N is the total number of unit cells in the crystal and $\delta(\boldsymbol{k} - \boldsymbol{\tau})$ is the "delta function" with $\boldsymbol{\tau}$ being a reciprocal lattice vector. The summation is carried out over all reciprocal lattice vectors $\boldsymbol{\tau}$. Thus scattering occurs for scattering vectors $\boldsymbol{k}$ which correspond to a reciprocal lattice vector and with an intensity which is determined by the square of the modulus of the nuclear structure factor $F_N(\boldsymbol{\tau})$. In actual experiments the Bragg reflection will not be such a sharp peak as indicated by the "delta function" in (4). Peak broadening occurs due to the resolution of the instrument and also due to sample characteristics (e.g. as given by the spatial extent of the coherently scattering regions in the sample). However, the details of the peak shape are not of interest here, and there is no need to pursue this point any further. The integrated Bragg intensity for a Bragg reflection characterised by $\boldsymbol{\tau}$ is given by

$$I(\boldsymbol{\tau}) = S(\boldsymbol{\tau}) \cdot |F_N(\boldsymbol{\tau})|^2 . \tag{5}$$

$S(\boldsymbol{\tau})$ is a reflection dependent scaling factor. The scattering vector dependence of S arises due to the method used to integrate the Bragg peaks. The geometric correction is known as the Lorentz correction, and it is readily eliminated from the measured integrated intensities. There remains an overall scale factor which is scattering vector independent. The scale factor is proportional to N, the total number of unit cells in the crystal.

Denoting the new scale factor (after the elimination of the scattering vector dependence) by $\tilde{S}$, the experimentally determined integrated intensity of the Bragg reflection is given by

$$\tilde{S} \cdot |F_N(\boldsymbol{\tau})|^2 . \tag{6}$$

Up to a constant the measured intensities are therefore determined by the square of the nuclear structure factor. However, for the description of the nuclear structure the value of $F_N(\boldsymbol{\tau})$ is required. As pointed out above, for structures with an inversion centre of symmetry the nuclear structure factor may be chosen real. Thus solving the nuclear structure reduces to choosing, for each reflection, the "correct" sign in the equation

$$F_N(\boldsymbol{\tau}) \approx \pm\sqrt{I(\boldsymbol{\tau})} = \pm\sqrt{\tilde{S} \cdot |F_N(\boldsymbol{\tau})|^2} . \tag{7}$$

It is pointed out that solving the above phase problem for all reflections is equivalent to the determination of the atomic positions in the unit cell. This is so because having obtained the structure factors $F_N(\boldsymbol{\tau})$ for a sufficient number of

reflections, the atomic positions may be obtained by Fourier inversion. Writing (3) in the form

$$F_N(\tau) = \int_{\substack{\text{unit}\\ \text{cell}}} \left(\sum_i b_i \delta(r - R_i) \right) e^{i\tau \cdot r} dr \tag{8}$$

it is seen that the nuclear structure factor is nothing else but the Fourier transform of the interaction potential, which in turn is determined by the positions of the atoms and their scattering strengths.

The above derivation was carried out using some simplifying assumptions. The lattice has been taken as perfect, and the thermal motion of the atoms has been neglected. The temperature motion and zero point fluctuations can be taken into account by the substitution

$$b_i \rightarrow b_i e^{-W(k)k^2}, \tag{9}$$

where $W(k)$ is the temperature factor which may be anisotropic. The function $\exp(-W(k)k^2)$ is known as the Debye–Waller factor. Other experimental factors such as extinction and absorption corrections are also readily applied [5], and standard procedures exist for taking these into account [6].

2.2. Magnetic scattering

In comparison to nuclear scattering, for which the interaction potential between neutron and nucleus is determined by the nuclear force, magnetic scattering of neutrons is based on an entirely different interaction mechanism. Magnetic neutron scattering referred to here arises due to an electromagnetic interaction between the magnetic dipole moments of the neutron and those of the electrons. An introduction and a complete derivation of the basic formulae for magnetic neutron scattering can be found in standard text books on neutron scattering [1, 2].

Here the interest is focused on elastic magnetic scattering only, with the magnetic structure being restricted to ferromagnetic order. For the purpose of carrying out the neutron scattering experiment it is immaterial whether the ferromagnetic order is intrinsic or whether it has been induced by the application of an external magnetic field.

A more detailed analysis (as given, e.g., in [1, 2, 4]) shows that the strength of the neutron–electron magnetic moment interaction is determined by the product of the gyromagnetic ratio of the neutron γ ($\gamma = -1.913$) and the classical electron radius r_0 with $r_0 = 2.81785 \times 10^{-15}$ m. The product $b_M = \gamma r_0 = -5.39 \times 10^{-15}$ m defines a magnetic scattering length b_M, which provides the unit for measuring the strength of magnetic moments in magnetic neutron scattering experiments. Therefore in the following the magnetic moments μ will always be measured in units of b_M. It is also important to note here that the magnitude of b_M is comparable with typical magnitudes of nuclear scattering lengths.

For a ferromagnetically ordered state the cell dimensions as defined by the chemical unit cell are not changed. Hence by summing over the same atoms as in (3) a magnetic structure factor of the unit cell may be defined as

$$F_M(k) = \sum_i \mu_i f_i(k) e^{ik \cdot R_i}. \tag{10}$$

Here μ_i is the magnetic moment located on the i-th atom, and $f_i(k)$ is the atomic magnetic form factor of the atom. The form factor f_i is normalised according to

$$f_i(\tau = 0) = 1. \tag{11}$$

The magnetic structure factor as defined in (10) is a vector quantity. The overall strength of the magnetic neutron scattering is determined by the sizes of the magnetic moments. Atoms with no magnetic moment, $\mu_i = 0$, will not contribute to the magnetic scattering. An additional scattering vector dependence is introduced into the structure factor due to the magnetic form factor. In general, the magnetic form factor tends to decrease with increasing magnitude of the scattering vector. As a consequence, the magnetic scattering diminishes for increasing scattering angles. This is in contrast to nuclear scattering for which the equivalent nuclear form factor is independent of the scattering vector and equal to one.

Similarly to the case of the structure factor for nuclear scattering the magnetic structure factor can be expressed as the Fourier transform of the interaction potential. For magnetic scattering the interaction potential is given by the magnetization density within the unit cell

$$F_M(k) = \int_{\substack{\text{unit}\\ \text{cell}}} M(r) e^{ik \cdot r} dr, \tag{12}$$

where $M(r)$ is the position dependent magnetization. $M(r)$ is a periodic function which has the periodicity of the nuclear lattice for a ferromagnetically ordered state. For a magnetization distribution which is given as the superposition of localised atomic magnetic moments located at r_i within the unit cell the magnetization density is given by

$$M(r) = \sum_i m_i(r - r_i). \tag{13}$$

In this case the magnetic structure factor in (12) reduces to

$$F_M(k) = \int \sum_i m_i(r - r_i) e^{ik \cdot r} dr. \tag{14}$$

A comparison with (10) yields the atomic form factor in the form

$$f_i(k) = \frac{1}{\mu_i} \int |m_i(r)| e^{ik \cdot r} dr \tag{15}$$

as the Fourier transform of the real space atomic magnetization $m_i(r)$. The total magnetic moment μ_i is defined as the integral of $m_i(r)$ according to

$$\mu_i = \int m_i(r) dr. \tag{16}$$

This definition together with (15) ensures the normalization of the atomic form factor as defined in (11). For localised moments the integration in (14) and (15) is carried out over the whole of the three-dimensional space. All the various magnetic contributions of each individual atom are subsumed within m_i. In general, m_i is composed of several magnetic moments, including spin and orbital magnetic contributions and, if necessary, a core polarization as well.

For the case of itinerant electron magnetism, for which the electronic wave functions are sufficiently delocalised, the general form (12) has to be used for

the description of the magnetic structure factor. In general, it is not possible to uniquely allocate a given magnetization density to an individual atom, and the notion of a magnetic moment located on an atom loses its meaning. It is only meaningful to talk about the total magnetic moment per unit cell, M_{tot}, with the total magnetic moment being defined as

$$M_{\mathrm{tot}} = \int_{\substack{\mathrm{unit}\\ \mathrm{cell}}} \mathrm{M}(r)\mathrm{d}r. \tag{17}$$

Obviously for the case of localised magnetic moments M_{tot} is determined by the sum over all magnetic moments in the unit cell.

In this way the magnetic structure factor may be defined for both, localised as well as itinerant electron magnetism. However, for neutron scattering additional complications arise due to the vector form of the magnetic structure factor as compared to an equivalent scalar quantity for nuclear scattering.

It turns out [1, 2, 4] that only those components of $\boldsymbol{F}_M(k)$ which are perpendicular to the scattering vector k may give rise to magnetic neutron scattering. The components which are active in the scattering process are defined as

$$\boldsymbol{F}_M^{\perp}(k) = \frac{1}{|k|^2} k \times (\boldsymbol{F}_M(k) \times k). \tag{18}$$

In order to combine the magnetic scattering contribution as defined by the vector in (18) with the nuclear scattering part as described by the scalar quantity $F_N(\tau)$ the vector $\boldsymbol{F}_M^{\perp}(k)$ has to be reduced to a scalar. A more detailed analysis shows that it is the scalar product of $\boldsymbol{F}_M^{\perp}(k)$ with the polarization vector $\boldsymbol{P}$ of the neutron beam that is needed for the neutron scattering cross-section. The scalar magnetic structure factor is defined as

$$F_M^{\perp}(k) = \boldsymbol{P} \cdot \boldsymbol{F}_M^{\perp}(k). \tag{19}$$

For perfect polarization of the neutron beam $\boldsymbol{P}$ is a unit vector, the direction of which indicates the polarization direction. For a partial polarization of the neutron beam $|\boldsymbol{P}|$ is defined as

$$|\boldsymbol{P}| = \left| \frac{n_\uparrow - n_\downarrow}{n_\uparrow + n_\downarrow} \right| \tag{20}$$

with $n_\uparrow$, $n_\downarrow$, being the number of spin up or spin down neutrons in the beam. $\boldsymbol{F}_M^{\perp}(k)$ is the entity which plays the equivalent role to the nuclear structure factor in the formula for the scattering cross-section. For this reason $\boldsymbol{F}_M^{\perp}(k)$ will be referred to as the magnetic structure factor. (This should not be confused with $\boldsymbol{F}_M(k)$ as defined in (10).) Considering only magnetic scattering, the differential cross-section is determined as

$$\frac{\mathrm{d}\sigma}{\mathrm{d}\Omega}(k) = N_M \sum_{\tau_M} |F_M^{\perp}(k)|^2 \delta(k - \tau_M), \tag{21}$$

where τ_M is a reciprocal lattice vector of the magnetic lattice and N_M is given by the number of magnetic unit cells in the sample. For ferromagnetic order the chemical and magnetic unit cells are identical. Consequently N_M and τ_M have the same values as their nuclear counterparts.

With nuclear and magnetic scattering present both contributions have to be combined. There are the two possibilities of either combining the intensities of nuclear and magnetic scattering or of adding the structure factors first and then inserting the sum into the formula for the differential cross-section.

For the first possibility the intensities are summed by adding (4) and (20). This corresponds to an incoherent superposition of the scattered waves from the nuclear and the magnetic subsystems of the target. Here, however, nuclear and ferromagnetic scattering is considered which is superimposed on the same Bragg reflection. Under these conditions it is the sum of the nuclear and the magnetic structure factors as determined by (3), (14) and (19), which has to be evaluated. The underlying assumption is one of a coherent superposition of nuclear and magnetic scattering contributions. The sum has to be inserted into the expression for the differential cross-section. Assuming perfect polarization of the neutron beam one arrives at

$$\left(\frac{\mathrm{d}\sigma}{\mathrm{d}\Omega}(k)\right)_{\uparrow\uparrow} = N\sum_{\tau}|F_N(k)+F_M^{\perp}(k)|^2\delta(k-\tau), \tag{22a}$$

$$\left(\frac{\mathrm{d}\sigma}{\mathrm{d}\Omega}(k)\right)_{\uparrow\downarrow} = N\sum_{\tau}|F_N(k)-F_M^{\perp}(k)|^2\delta(k-\tau) \tag{22b}$$

for a neutron spin polarization parallel (a) and antiparallel (b) to the external magnetic field direction. For a partially polarised neutron beam the cross-section is an average of (22a) and (22b) with the weighing factors determined by the proportion of spin up and spin down neutrons in the neutron beam. For this case the cross-section takes the form

$$\left(\frac{\mathrm{d}\sigma}{\mathrm{d}\Omega}(k)\right)_{\text{polarization}\,\boldsymbol{P}} = N\sum_{\tau}\left(|(F_N(k)|^2+2F_N(k)\boldsymbol{P}\cdot\boldsymbol{F}_M^{\perp}+F_M^{\perp 2}\right)\delta(k-\tau). \tag{23}$$

The direction of $\boldsymbol{P}$ is taken to be parallel to the direction of the external magnetic field. This form of the differential neutron scattering cross-section differs by the presence of an interference term between nuclear and magnetic scattering from the cross-section obtained for an incoherent superposition of the nuclear and magnetic intensities. The incoherent superposition is realized for an unpolarised neutron experiment, for which the magnitude of $\boldsymbol{P}$ is equal to zero. In this case the differential cross-section takes the form

$$\left(\frac{\mathrm{d}\sigma}{\mathrm{d}\Omega}(k)\right)_{\text{no polarization}} = N\sum_{\tau}(|F_N(k)|^2+|F_M^{\perp}(k)|^2)\delta(k-\tau). \tag{24}$$

It is the presence of the interference term between nuclear and magnetic scattering which forms the basis of magnetic form factor measurements. It depends on the polarization of the neutron beam through $\boldsymbol{P}$ in (23) or through the change of sign of $F_M^{\perp}$ in (22a) and (22b). In the next section it will be discussed how this interference is exploited experimentally and how it can be utilised for the investigation of details of the magnetization on an atomic level.

2.3. Experimental

The quantities which have to be determined by experiment are the nuclear and magnetic structure factors. These are measured in separate experiments and by using unpolarised and polarised neutrons, respectively.

The measurement of the nuclear structure factor is equivalent to a structure determination experiment. In the experiment the integrated Bragg intensity is determined for a number of Bragg reflections. As discussed above in Sec. 2.1, a structural model may be used to refine the free parameters of a model structure, thus obtaining the nuclear structure factors $F_N(\tau)$ for all Bragg reflections used in the refinement. The nuclear structure factor together with other experimental entities such as lattice parameter etc. are assumed known when the spin polarised neutron experiment is carried out.

For the determination of the magnetic form factor a single crystal of the material under investigation is orientated in an external magnetic field in such a way that the magnetic moment is along the magnetic field direction. This necessitates that the magnetic field is directed parallel to an easy axis of magnetization. In order to maximize the magnetic signal (see (18)) it is preferable to align the magnetic field perpendicular to the scattering plane (which is defined as the plane spanned by the wave vectors of the incoming and scattered neutrons with the scattering vector being the difference of these two vectors). Spin polarised neutrons are used in the form factor measurement. However, no polarization analysis is needed after the neutrons are Bragg scattered by the sample under investigation.

For a given Bragg reflection τ and assuming a perfect neutron spin polarization the differential neutron scattering cross-sections are determined to be

$$\left(\frac{\mathrm{d}\sigma}{\mathrm{d}\Omega}(k)\right)_{\uparrow\uparrow} = N \sum_{\tau} \left|F_N(k) + F_M^{\perp}(k)\right|^2 \delta(k-\tau), \tag{25a}$$

$$\left(\frac{\mathrm{d}\sigma}{\mathrm{d}\Omega}(k)\right)_{\uparrow\downarrow} = N \sum_{\tau} \left|F_N(k) - F_M^{\perp}(k)\right|^2 \delta(k-\tau). \tag{25b}$$

The integrated intensities of this Bragg reflection are given by

$$I_{\uparrow\uparrow} = S(\tau) \left|F_N(\tau) + F_M^{\perp}(\tau)\right|^2, \tag{26a}$$

$$I_{\uparrow\downarrow} = S(\tau) \left|F_N(\tau) - F_M^{\perp}(\tau)\right|^2. \tag{26b}$$

Here $\uparrow\uparrow$ denotes a neutron spin polarization parallel to the applied magnetic field, while $\uparrow\downarrow$ indicates an antiparallel neutron spin polarization.

By using either the differential cross-section of the integrated Bragg intensity the flipping ratio $R(\tau)$ is defined as

$$R(\tau) = \frac{\left(\frac{\mathrm{d}\sigma(\tau)}{\mathrm{d}\Omega}\right)_{\uparrow\uparrow}}{\left(\frac{\mathrm{d}\sigma(\tau)}{\mathrm{d}\Omega}\right)_{\uparrow\downarrow}} = \frac{I_{\uparrow\uparrow}}{I_{\uparrow\downarrow}} = \left|\frac{F_N(\tau) + F_M^{\perp}(\tau)}{F_N(\tau) - F_M^{\perp}(\tau)}\right|^2. \tag{27}$$

Experimentally it is easier and faster to measure the relative intensities of spin up and spin down neutrons at only one point on the Bragg reflection (which in the experiment is found to be broadened to a Gaussian peak shape compared to

a "delta function" indicated in the above formulae) instead of having to obtain the integrated intensities for both neutron spin orientations. Therefore, in the experiment the crystal is set so as to maximize the counting rate for a given Bragg reflection and the relative counting rates are measured as determined by (25a) and (25b). To the extent that the shapes of the nuclear and magnetic Bragg reflections are identical $R(\tau)$ does not depend on how the ratio is defined, whether by using the ratio of the integrated intensities or by utilizing the ratio at only one point of the Bragg reflection. As discussed in detail elsewhere [5], other experimental factors are readily included in the definition of the flipping ratio. Taking into account a partial polarization P of the neutron beam, the efficiency e of the neutron spin flipper and the angle Θ between magnetic moment direction and scattering vector, the flipping ratio takes the form

$$R(\tau) = \left| \frac{F_N^2(\tau) + 2P\sin^2\Theta F_N(\tau)F_M(\tau) + \sin^2\Theta F_M^2(\tau)}{F_N^2(\tau) - 2Pe\sin^2\Theta F_N(\tau)F_M(\tau) + \sin^2\Theta F_M^2(\tau)} \right|. \tag{28}$$

Returning to the expression of the flipping ratio as given in (27), the equation is readily inverted to yield the ratio of the magnetic to nuclear structure factors as a function of the flipping ratio

$$\frac{F_M^{\perp}(\tau)}{F_N(\tau)} = \frac{[R(\tau)+1] \pm 2\sqrt{R(\tau)}}{R(\tau)-1}. \tag{29}$$

The ambiguity given by the $\pm 2\sqrt{R(\tau)}$ term in (29) is related to the ambiguity of writing $R(\tau)$ in (27) either in terms of $F_M^{\perp}/F_N(\tau)$ or by using the inverse ratio $F_N(\tau)/F_M^{\perp}(\tau)$. It is the equivalent to the question of whether $F_M^{\perp}(\tau)/F_N(\tau)$ is larger or smaller than one. In an actual experiment this does generally not present a problem, because a choice can be made on physical grounds.

At this point it is worth stressing again that the knowledge of the nuclear structure factor is vital for the determination of $F_M^{\perp}(\tau)$. The uncertainty in the magnetic structure factor is firstly determined by the experimental error in the measurement of the flipping ratio $R(\tau)$, but secondly also, and more importantly, by the uncertainty in the nuclear structure factor. As seen from (29) the magnetic structure factor is measured in units of the nuclear one, and consequently any systematic error in the determination of the nuclear structure factor (as given by the neglect of temperature factors, absorption, extinction etc.) will influence the accuracy of the magnetic structure factor.

Some particular features of the flipping ratio are worth noting. It is first of all a quantity which is independent of a scaling factor. By taking the ratio in (27) the scaling factors have cancelled. Furthermore, it is a function only of the nuclear and the magnetic structure factors.

To appreciate the significance of this statement consider the case of weak ferromagnetic order characterised by

$$|F_M^{\perp}(\tau)| \ll |F_N(\tau)|. \tag{30}$$

When expanding (27) to leading order in $F_M^{\perp}(\tau)/F_N(\tau)$ the flipping ratio is given by

$$R(\tau) \approx 1 + 4F_M^{\perp}(\tau)/F_N(\tau). \tag{31}$$

The deviation of the flipping ratio from one is a direct measure of the magnitude of $F_M^{\perp}$ as measured in units of the nuclear structure factor. As $F_N(\tau)$ is known from a previous structure determination experiment the deviation of the flipping ratio from one immediately yields the value of $F_M^{\perp}(\tau)$: both its *magnitude and phase!* (It should be stressed again that only centrosymmetric structures are considered here. For such structures the phase degree of freedom of the structure factors reduces to a choice of a $\pm$ sign in front of the wave function.)

In these respects the measurement of the flipping ratio is unusual. It renders possible an absolute measurement without the necessity of a normalization. Furthermore, it allows for a simultaneous determination of the amplitude and the phase of the magnetic scattering contribution. The physical origin of this can be traced back to the presence of the interference term in the differential neutron scattering cross-section. As the interference term is proportional to the product of the nuclear and magnetic structure factors the phase of the magnetic scattering can be related to the phase of the nuclear structure factor. The phase problem for the nuclear structure factor (which is the key question for any structure determination) has been solved and the phase is already determined (up to an overall phase factor common to all reflections). Thus the knowledge of the phase of the nuclear structure factor can be used to extract the information on the phase of the magnetic structure factor.

It is also worth pointing out that due to the interference term the sensitivity is significantly increased. While for an experiment employing unpolarised neutrons and with ferromagnetic order present in the sample the scattered intensity is given by

$$I \approx F_N^2(\tau) + F_M^2(\tau) = F_N^2(\tau)[1 + F_M^2(\tau)/F_N^2(\tau)], \tag{32}$$

for an experiment carried out with spin polarised neutrons the intensity change is determined to be given by

$$I \approx [F_N(\tau) + F_M^{\perp}(\tau)]^2 = F_N^2(\tau)[1 + F_M^{\perp}(\tau)/F_N(\tau)]^2$$

$$\approx F_N^2(\tau)[1 + 2F_M^{\perp}(\tau)/F_N(\tau)] + \ldots \tag{33}$$

For a ratio of $F_M^{\perp}(\tau)/F_N(\tau) = 0.1$, the change of intensity, $\delta I/I$, may be compared with and normalized to the intensity I of an identical sample without magnetic order. For an unpolarised neutron experiment $\delta I/I$ is of order 1%, while a value of order 20% is found for $\delta I/I$ for the spin polarised neutron scattering experiment. This increased sensitivity in spin polarised neutron scattering experiments allows for a more accurate determination of the magnetic scattering contribution and, finally, also of the magnetic structure factor.

Thus, a measurement of the flipping ratios yields accurate values of the magnetic structure factors. As an experimentally determined entity the magnetic structure factors are model independent. However, the collection of values of magnetic structure factors is not very revealing if presented on its own and in tabular form. It is more informative to consider the Fourier transform of the magnetic structure factors.

As pointed out above the magnetic structure factors are determined by the Fourier transformation of the magnetic interaction potential. According to (12)

the magnetic structure factor $F_M(\tau)$ is determined by

$$F_M(\tau) = \int_{\substack{\text{unit}\\ \text{cell}}} M(r)e^{i\tau \cdot r}dr. \tag{12}$$

The inverse transformation is given by

$$M(r) = \frac{1}{V}\sum_{\tau} F_M(\tau)e^{-i\tau \cdot r} \tag{34}$$

with V being the volume of the unit cell. The summation is carried out over all reciprocal lattice vectors τ. The magnetic structure factors are the Fourier coefficients in the series (34). The Fourier transform back into real space will therefore construct a picture of the real space interaction potential, which amounts here to the magnetization density distribution. In this manner a map of the magnetization density may be constructed and presented in real space as either a cut through the unit cell or as a projection.

In order to be able to perform the Fourier transformation by using the experimentally determined magnetic structure factors an infinite number of the Fourier components in (34) has to be known. Experimentally this presents a problem, as only a finite number of coefficients can be determined. A Fourier series is an infinite series and it is only complete if all coefficients of the infinite series are included. Therefore, constructing a magnetization map by using a finite subset of coefficients will result in "incomplete" and thus erroneous magnetization density maps. However, it turns out that a magnetization density map constructed by using a finite set of coefficients in (34) may still be meaningful and yields a magnetization density with the important features present. In order to understand the limitations imposed by the finite number of magnetic structure factors and to appreciate the significance of magnetization density maps a more detailed discussion of some of the relevant aspects is helpful. A discussion relating to these questions has been given by Moon [7].

A reflection which is not measurable by neutrons is the Bragg reflection corresponding to $\tau = 0$. However, for this reciprocal lattice vector the definition of the magnetic structure factor in (12) reduces to the evaluation of the total magnetic moment in the unit cell as given in (17). While this reflection is not accessible in the neutron scattering experiment, its value may be obtained by magnetization measurements using conventional magnetometers. Its inclusion in the Fourier series and in a magnetization density map adds a scattering vector independent contribution. This Fourier coefficient may thus be considered to fix the zero level in the magnetization density map.

A more serious limitation is the upper cut-off in $|\tau|$ in the summation of the Fourier series. Denote by k_c the magnitude of the scattering vector τ beyond which no more experimental values of $F_M^{\perp}(\tau)$ are available. k_c is taken to characterise the upper limit of the cut-off in the Fourier series. The coefficients belonging to $|\tau| > k_c$ give rise to fast oscillating contributions in the unit cell. These components are needed for the description of the finer details in the magnetization density in real space. By not including these magnetic structure factors in (34) these details are lost. This loss of detailed structure corresponds to a picture where in the

perfect real space magnetization density (which is obtained by including all Fourier coefficients in (34)) a local average is carried out over a small volume element so as to eliminate the fast oscillating contributions within this volume element. In order to estimate the dimension of the volume element and to be able to relate it to k_c the following procedure may be used (it suffices to consider the one-dimensional case). The magnitude of the cut-off wave vector k_c defines a characteristic length in reciprocal space. Let r_c be a characteristic length in real space. A reasonable estimate for the interval of average $[0, r_c]$ will be given by a value of r_c for which the phase factor $\exp(i\boldsymbol{k} \cdot \boldsymbol{r})$ undergoes several (but at least one) oscillation(s) as r is varied within the limits of the averaging interval and for a scattering vector $k > k_c$. This criterion results in a definition of r_c given by $k_c \cdot r_c = 2\pi$. Writing k_c in terms of a cut-off scattering angle Θ_c as $k_c = 4\pi \sin\Theta_c/\lambda$, with λ being the neutron wavelength employed in the experiment, the interval of average is defined as $\left[0, \frac{1}{2}\frac{\lambda}{\sin\Theta_c}\right]$. For the two- or three-dimensional cases the volume of average may be taken to be a square or a cube with the linear dimensions defined by r_c.

Thus carrying out a Fourier transform on a limited set of Fourier coefficients may still yield a correct magnetization density which, however, is deprived of some details in its structure. The experimentally determined magnetization densities are therefore not sensitive on a length scale defined by r_c, with the fine structure being smeared out over the average volume.

The coefficients which remain in (34) are all those Fourier components which belong to scattering vectors τ with $|\tau| < k_c$. It is obvious that within this limited range the set of coefficients must be complete, or at least as complete as possible, for a meaningful magnetization picture to emerge from the Fourier transformation. As the various Fourier components in (34) are linearly independent a "missing component" in the series cannot be compensated by other ones. A magnetization density map will be severely distorted when constructed with an incomplete finite series with some coefficients missing for a τ with $|\tau| < k_c$. An example of a magnetization density map with a missing component will be given below.

So far the discussion has been restricted to a paramagnetic material with a centrosymmetric crystallographic structure, and the procedures of a magnetic form factor measurement have been developed within this restriction. In order to complete this section, a brief discussion is given of the problems which arise when these restrictions are lifted.

First, consider a magnetically ordered state of the sample. A brief but very instructive introduction to the investigation of magnetic order by neutron scattering has been given by Brown [8]. The crystallographic structure is still required to be centrosymmetric. For a ferromagnetically ordered sample a magnetic field is not needed for inducing magnetic moments or aligning disordered ones, because long-range ferromagnetic order is assumed present. However, in order to define a unique direction of the magnetic moment, and thus $F_M^{\perp}(\tau)$, an external magnetic field has to be applied. This is true even in the case of strong magnetic anisotropy, which tends to align the moments along a given crystallographic axis. Under these circumstances the external magnetic field has to remove the degeneracy connected with the domain structure in the magnetically ordered state. Only if the whole sin-

gle crystal is also characterised by only one magnetic domain the approximations do apply in the derivation of the flipping ratio in (27). It has already been pointed out above that in the case of magnetic anisotropy the external magnetic field must be applied parallel to an easy axis of magnetization. All these precautions have to be taken in order to uniquely define the direction of magnetic moments in the crystal under investigation.

For the case of an antiferromagnetically ordered structure the measurement of the magnetic form factor is complicated due to several factors. For many antiferromagnetic structures the magnetic order changes the size of the unit cell. As a result, magnetic and nuclear Bragg reflections occur at different points in reciprocal space. For a magnetic form factor measurement, however, the presence of nuclear and magnetic scattering is needed at the same reciprocal lattice point. If a nuclear reciprocal lattice vector τ_{nuclear} does not coincide with a τ_{magnetic}, the nuclear-magnetic interference term will be absent from the elastic neutron scattering cross-section. Thus an interference term in the elastic neutron scattering cross-section will be absent for antiferromagnetic structures with an increased unit cell volume due to the magnetic order. This does also include more complicated magnetic structure such as incommensurate or helical ones.

Therefore, only the case of an antiferromagnet without an increased unit cell needs to be considered further. Such an antiferromagnetic order occurs, for example, in a bcc structure where the magnetic atoms at positions (0, 0, 0) and (1/2, 1/2, 1/2) have their magnetic moments aligned antiparallel with respect to one another.

The various cases of magnetic ordering are best described with the help of the time inversion operator $\hat{\Theta}_t$. When acting on a magnetic moment M this operator reverses the moment direction according to

$$\hat{\Theta}_t M = -M. \tag{35}$$

In addition to the time inversion operator $\hat{\Theta}_t$ it is only the symmetry element for the inversion in space, I, which is needed out of all the symmetry elements which characterise the crystallographic structure. Space inversion does not change the orientation of the magnetic moment M. (This is due to the fact that the spin part of the magnetic moment is not coupled to the spatial coordinates, while the orbital part of M is proportional to the pseudovector $r \times p$, where r is the position of the electron under consideration and p is its linear momentum. The vector product $r \times p$ does not change its orientation when acted upon by I.) For ferromagnetic order and some antiferromagnets the inversion symmetry operator is not combined with the time inversion. As a consequence any atom at position R_i has an equivalent atom located at $-R_i$. Thus grouping those atoms together which are related by inversion symmetry, their contribution to the magnetic structure factor is found to be proportional to

$$F_M(\tau) \propto M_i e^{i\tau \cdot R_i} + M_i e^{-i\tau \cdot R_i} = 2M_i \cos(\tau \cdot R_i). \tag{36}$$

As seen from (36) under the above assumptions the magnetic structure factor is a real quantity. (This was assumed above and stated without proof for the magnetic structure factor of the paramagnet in an external magnetic field.)

If, however, the antiferromagnetic state is characterised by a combination of operators as given by the product of space inversion times time inversion symmetry operator, the magnetic moment of the symmetry related atom is reversed. This results in a magnetic structure factor proportional to

$$\boldsymbol{F}_M(\boldsymbol{\tau}) \propto \boldsymbol{M}_i e^{i\boldsymbol{\tau}\cdot\boldsymbol{R}_i} - \boldsymbol{M}_i e^{-i\boldsymbol{\tau}\cdot\boldsymbol{R}_i} = 2i\boldsymbol{M}_i \sin(\boldsymbol{\tau}\cdot\boldsymbol{R}_i). \tag{37}$$

This magnetic structure factor is purely imaginary. It is phase shifted by 90° with respect to the nuclear structure factor. As a consequence of this phase shift the flipping ratio as defined in (27) is identically equal to one. Denoting the real and imaginary part of the structure factor by Re and Im, respectively, and under the assumption as stated above that the structure factors are given by

$$F_N(\tau) = \mathrm{Re}(F_N(\tau)), \qquad F_M^{\perp} = i\,\mathrm{Im}(F_M^{\perp}(\tau)). \tag{38}$$

The flipping ratio as defined in (27) is equal to one for all reflections τ because the identity

$$|\mathrm{Re}(F_N(\tau)) + i\,\mathrm{Im}(F_M^{\perp}(\tau))| = |\mathrm{Re}(F_N(\tau)) - i\,\mathrm{Im}(F_M^{\perp}(\tau))|$$

$$= |F_M(\tau) + F_M^{\perp}(\tau)| = |F_N(\tau) - F_M^{\perp}(\tau)| \tag{39}$$

is fulfilled for all Bragg reflections. Therefore no $R(\tau) \neq 1$ reflection may be found for an antiferromagnetic structure which combines the space inversion element with time inversion.

However, for a structure for which the space inversion element is a proper symmetry element both the nuclear and magnetic structure factors are real quantities. This is the case for a ferromagnetic and some types of antiferromagnetic structure, for which the assumptions leading to (36) are true. Only for these structures a measurement of the flipping ratio is a possibility.

However, in addition to the structural requirements which have to be fulfilled for a nonzero flipping ratio to occur, a further complication arises due to the presence of magnetic domains in the sample. For most magnetic structures and including a coupling to the lattice a small number of magnetic domains is possible. It suffices here to restrict the discussion to two domains, which are related to one another by time inversion symmetry. Such a pair of magnetic domains is always possible. It is appropriate to denote these domains as a 0° and a 180° domain, because the 180° domain is obtained from the 0° domain by an inversion of all magnetic moment directions. It may also be described as obtaining the 180° domain from the 0° one by the action of Θ_t on the 0° domain.

Both domains are energetically degenerate. It may therefore be expected that the two domains occur with the same probability in a sample. Therefore, the magnetic structure factor of the whole sample has to be obtained by averaging over the various magnetic domains. This average, however, will result in a zero average magnetic structure factor.

With the definition of the magnetic structure factor as given in (12) and by using an obvious notation to identify the structure factors for the various magnetic domains one obtains

$$\boldsymbol{F}_M^{\perp}(\boldsymbol{\tau})\Big|_{0°\text{domain}} = -\,\boldsymbol{F}_M^{\perp}(\boldsymbol{\tau})\Big|_{180°\text{domain}} \tag{40}$$

The magnetic structure factor is a vector, the direction of which is determined by the direction of the magnetic moments. As the magnetic moment direction is reversed by going from one domain to the other the magnetic structure factor changes sign. Therefore, a zero average magnetic structure factor results for any sample with equal amounts of magnetic domains present which are related by time inversion symmetry. This argument applies equally well for a ferromagnetically as well as an antiferromagnetically ordered structure.

In order to remove the degeneracy of the 0° and 180° magnetic domains a magnetic field has to be applied. For a ferromagnetically ordered sample it suffices to apply a homogeneous external magnetic field. This field removes the degeneracy of the magnetic domains, and if of sufficient strength it may stabilize a single magnetic domain in the whole crystal.

For an antiferromagnet the applied magnetic field has to have the modulation of the antiferromagnetic structure in order to remove the degeneracy. The wave vector of the magnetic modulation is of the order of angströms, and at present no externally applied magnetic fields are available with such short wavelengths. Other experimentally controlled parameters such as pressure do not break time inversion symmetry, and they are therefore not capable of removing the degeneracy of the magnetic domains.

Thus one is left with the conclusion that for an antiferromagnetic structure a flipping ratio may be observed for certain structures and under the condition of an imbalance of magnetic domains which are related by time inversion symmetry. The above discussion has illustrated the complexity of the argument and it has borne out the experimental difficulties which have to be overcome.

Not withstanding these problems measurements of the flipping ratio in an antiferromagnetic structure have successfully been carried out [9]. The interested reader is referred to the original publications for a detailed discussion of various aspects of the experiment.

For an antiferromagnetically ordered substance an external magnetic field may be applied to induce a ferromagnetic component. This may be achieved by tilting the magnetic moments out of their antiparallel alignment into the direction of the external magnetic field thereby creating a ferromagnetic component. This situation is illustrated in Fig. 1. The ferromagnetic component of the magnetic structure is characterised by a wave vector $k_0 = 0$, while the antiferromagnetic component is described by a wave vector q. It is only the k_0 component which couples to an applied magnetic field. The contributions of both wave vectors may be decoupled and considered separately. For the ferromagnetic component the theory applies as developed above. For the antiferromagnetic component all those complications arise which have been considered in the earlier discussion. In the experiment proper account has to be taken of both magnetic components. Thus, in a form factor measurement of an antiferromagnetic crystal (which does not increase the dimensions of unit cell by ordering antiferromagnetically) and which is placed in an external magnetic field it is only the ferromagnetic component which contributes to the interference term. However, due account has to be taken of the antiferromagnetic scattering contribution to the total intensity of the Bragg peak.

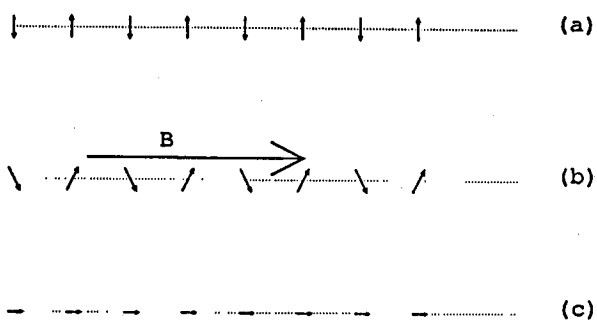

Fig. 1. Figure 1 shows the arrangement of spins for an antiferromagnetically ordered structure (a). If a moderately strong and homogeneous field is applied as shown in part (b), the spin on each atom is tilted slightly into the direction of the applied magnetic field. The resulting arrangement of spins (part (b)) may be resolved into an antiferromagnetic (part (a)) and a ferromagnetic (part (c)) contribution.

For crystallographic structures which do not possess a centre of inversion symmetry the nuclear and magnetic structure factors are complex quantities. This implies a larger number of components for their characterization. One complex number, or equivalently two real numbers to characterise real and imaginary parts, are needed as compared to only one real number and a sign in the case of centrosymmetric structures. The generalization of the above derivation to non-centrosymmetric structures will result in more complicated expressions [5]. Denoting the real and imaginary parts by $'$ and $''$, respectively, and dropping the scattering vector dependence of the functions, the flipping ratio takes the form

$$R = \left| \frac{F_N' + \mathrm{i}F_N'' + \left(F_M^{\perp\prime} + \mathrm{i}F_M^{\perp\prime\prime}\right)}{F_N' + \mathrm{i}F_N'' - \left(F_M^{\perp\prime} + \mathrm{i}F_M^{\perp\prime\prime}\right)} \right|^2 . \tag{41}$$

While the nuclear structure factor $F_N' + \mathrm{i}F_N''$ is known, it suffices to note that a single measurement of only one flipping ratio per Bragg reflection is not sufficient for extracting the complex quantity $F_M^{\perp}(\tau)$. A second measurement is needed for which the external magnetic field direction or the orientation of the crystal is reversed.

As pointed out above the real part of the structure factor is related to that part of the magnetization which is symmetric with respect to the inversion operator. The imaginary part on the other hand is antisymmetric under space inversion. If the external magnetic field direction is reversed, the real part of the magnetic structure factor will not change its sign while the imaginary part will. Thus reversing the external field direction will yield a flipping ratio given by

$$R = \left| \frac{F_N' + \mathrm{i}F_N'' + \left(F_M^{\perp\prime} - \mathrm{i}F_M^{\perp\prime\prime}\right)}{F_N' + \mathrm{i}F_N'' - \left(F_M^{\perp\prime} - \mathrm{i}F_M^{\perp\prime\prime}\right)} \right|^2 . \tag{42}$$

For a non-centrosymmetric structure the flipping ratio is different for the two con-

figurations of the magnetic field. These two measurements are in general sufficient to determine both the real and the imaginary part of the magnetic structure factor. For a centrosymmetric structure the second setup will yield the same flipping ratio as the first measurement.

3. Magnetic form factor calculations for some simple model systems

In the previous section the magnetic form factor measurements have been considered from an experimental point of view. The magnetic structure factors and their Fourier transform in the form of magnetization density maps are the experimentally determined quantities. In order to fully interpret the experimental observation an attempt has to be made to quantitatively describe magnetization densities or magnetic structure factors. By using a model, parameters have to be obtained from observation for a description of the magnetization on an atomic level.

For the most general case the theory will be complicated, and the interested reader is referred to the literature for details of some theoretical aspects of neutron magnetic form factors (Harmon [10]). It will also not be attempted here to derive the full expressions for the magnetization in real space or of the wave vector dependent susceptibility (see e.g. Oh et al. [11], Cooke et al. [12]). Rather in order to illustrate the power of magnetic form factor measurements in this section attention will be focused on some simple model systems. The first case is characterised by delocalised or itinerant electrons, while a second model system is one with a collection of localised and atomic-like magnetic moments.

The theoretical evaluation of $M(r)$ necessitates the calculation of matrix elements of the form

$$M(r) = \langle \Psi | \widehat{M}(r) | \Psi \rangle, \tag{43}$$

where $|\Psi\rangle$ is the many-electron wave function of the crystal under investigation. Operators will here and henceforth be denoted by a $\hat{}$ sign in order to distinguish the operator from its expectation value.

Depending on the form of the operator it may be more convenient to present the wave function either in momentum space or in position space. These Hilbert spaces are defined such that the state vectors of the Hilbert space are either eigenstates of the linear momentum operator $\hat{p}$ with

$$\hat{p}|k\rangle = \hbar k|k\rangle \tag{44}$$

or of the position operator r as given by

$$\hat{r}|r\rangle = r|r\rangle. \tag{45}$$

The momentum space and the position space are assumed to be complete

$$\int \mathrm{d}k|k\rangle\langle k| = 1, \qquad \int \mathrm{d}r|r\rangle\langle r| = 1 \tag{46}$$

and the state vectors normalised

$$\langle k|k'\rangle = \delta(k - k'), \qquad \langle r|r'\rangle = \delta(r - r'). \tag{47}$$

The transformation which yields $|\Psi\rangle$ as either a representation in momentum or in position space is given by

$$|\Psi\rangle = \int \mathrm{d}k|k\rangle\langle k|\Psi\rangle = \int \mathrm{d}k\, u(k)|k\rangle,$$
$$|\Psi\rangle = \int \mathrm{d}r|r\rangle\langle r|\Psi\rangle = \int \mathrm{d}r\, u(r)|r\rangle \tag{48}$$

with the functions $u(k)$ and $u(r)$ being given as

$$u(k) = \langle k|\Psi\rangle, \qquad u(r) = \langle r|\Psi\rangle. \tag{49}$$

Within $u(k)$ and $u(r)$ is contained the information connected with the occupation of the various levels or energy bands of the solid. For a complete description of the quantum mechanical state both the state vectors and the functions $u(k)$ and $u(r)$ have to include an index σ to denote the electronic spin degree of freedom. The functions $u(k)$ and $u(r)$ are not independent from one another. The transformation of $u(k)$ from a momentum space representation to a position space representation is achieved by a Fourier transform.

For the magnetization operator $\widehat{M}(r)$ a separation is possible of the total magnetic moment operator into a spin and an orbital contribution according to

$$\widehat{M}(r) = \widehat{M}^S(r) + \widehat{M}^L(r). \tag{50}$$

Both the spin and the orbital contribution to the magnetization operator have a position dependence given by

$$\widehat{M}(r) = \widehat{M}\delta(\hat{r} - r) = \widehat{M}^S\delta(\hat{r} - r) + \widehat{M}^L\delta(\hat{r} - r). \tag{51}$$

For some magnetic materials the orbital component is zero. This may be the case either for a magnetic moment with $L = 0$ (with Mn^{2+} and Gd^{3+} being examples) or it may arise due to the quenching of the orbital moment due to crystalline electric fields. Examples of the latter are found among the $3d$ elements and their alloys. Under these conditions only the spin part of the magnetic moment operator is active. The operator for the spin density, $\widehat{M}^S(r)$, is defined as

$$\widehat{M}^S(r) = -2\mu_B \sum_i \hat{S}\delta(\hat{r} - r_i). \tag{52}$$

The summation is carried out over all electrons in the crystal. The spin operator $\hat{S}$ is determined as

$$\hat{S} = \frac{1}{2}(\hat{s}_\uparrow + \hat{s}_\downarrow)n, \tag{53}$$

where $\hat{s}_\uparrow$ and $\hat{s}_\downarrow$ are operators which distinguish between spin up and spin down states of the i-th electrons according to

$$\hat{s}_\uparrow|\uparrow\rangle = |\uparrow\rangle, \qquad \hat{s}_\downarrow|\uparrow\rangle = 0,$$
$$\hat{s}_\uparrow|\downarrow\rangle = 0, \qquad \hat{s}_\downarrow|\downarrow\rangle = -|\downarrow\rangle. \tag{54}$$

Here $|\uparrow\rangle$ and $|\downarrow\rangle$ denote the spin state of a single electron. The vector n is a unit vector which defines the axis of quantization in the system and a unique direction with respect to which the electron spins are either up or down.

Using the above definitions and transforming to a position space representation the matrix element (52) is evaluated to

$$M^S(r) = \langle\Psi|\widehat{M}^S(r)|\Psi\rangle = \int \mathrm{d}r' \int \mathrm{d}r''\langle\Psi|r'\rangle\langle r'|\widehat{M}^S(r)|r''\rangle\langle r''|\Psi\rangle. \tag{55}$$

The matrix element $\langle r'|\widehat{M}^S(r)|r''\rangle$ is readily evaluated with the result

$$\langle r'|\widehat{M}^S(r)|r''\rangle = -2\mu_B \sum_i \langle r'|\hat{S}\delta(\hat{r} - r_i)|\ r''\rangle$$

$$= -2\mu_B \sum_i S\langle r'|r''\rangle\delta(r'' - r_i) = -2\mu_B \sum_i S\delta(r' - r'')\delta(r'' - r_i). \tag{56}$$

On inserting (56) into (55) and integrating, the matrix element for the magnetization takes the form

$$M^S(r) = -2\mu_B \sum_i S|u_i(r)|^2. \tag{57}$$

The physical significance of this result can be made even more transparent when the spin variable is tranformed from S to the function $u_i(r)$. This is achieved in a similar manner as above in (53) by separating the spin up and spin down parts of $u_i(r)$ with the insertion of a spin index. The magnetization density can be written in the form

$$M^S(r) = -\mu_B \sum_i \left(\left|u_i^{\uparrow}(r)\right|^2 - \left|u_i^{\downarrow}(r)\right|^2\right) n$$

$$= -\mu_B \left(\overline{|u^{\uparrow}(r)|^2} - \overline{|u^{\downarrow}(r)|^2}\right) n. \tag{58}$$

The bar denotes the average spin up/spin down density of the electrons in the sample with the average being obtained by carrying out $\sum_i$ and summing over all electron contributions. This result shows that the magnetization density in real space is determined by the densities $\overline{|u^{\uparrow\downarrow}(r)|^2}$ of spin up and spin down electrons. A net magnetization arises at position r if the density of spin up electrons is different from the one of spin down electrons at this location in the crystal. Within this description no magnetic contribution arises for completely filled bands or atomic orbitals. Thus only those electronic wave functions may contribute to the magnetization density which belong to partially filled electronic bands or localised levels and which may give rise to a net magnetic moment.

As a special case and as an illustration of the discussion given above electrons are considered in a solid with their wave functions being given by those of free electrons. The quantum number k of these electrons is a good quantum number, yielding the free electron wave function in momentum space. It is therefore appropriate to re-evaluate the matrix element for the magnetization density in reciprocal space and by making use of the linear momentum representation for $|\Psi\rangle$.

According to (12) the Fourier transform of the magnetization density in real space is the magnetic structure factor. Thus

$$F_M^S(k) = \int \mathrm{d}r \langle \Psi | \widehat{M}^S(r) | \Psi \rangle \mathrm{e}^{\mathrm{i}k\cdot r}$$
$$= \int \mathrm{d}r \int \mathrm{d}k' \int \mathrm{d}k'' \langle \Psi | k' \rangle \langle k' | \widehat{M}^S(r) | k'' \rangle \langle k'' | \Psi \rangle \mathrm{e}^{\mathrm{i}k\cdot r}$$
$$= \int \mathrm{d}r \int \mathrm{d}k' \int \mathrm{d}k'' u^*(k') \langle k' | \widehat{M}^S(r) | k'' \rangle u(k'') \mathrm{e}^{\mathrm{i}k\cdot r}. \tag{59}$$

The index S on the magnetic structure factor indicates that it is only the spin part of the total magnetization which is included. With the help of the completeness relation (46) the matrix element $\langle k' | \widehat{M}^S(r) | k'' \rangle$ may be related to the matrix element in position space as given in (56):

$$\langle k' | \widehat{M}^S(r) | k'' \rangle = \int \mathrm{d}r' \int \mathrm{d}r'' \langle k' | r' \rangle \langle r' | \widehat{M}^S(r) | r'' \rangle \langle r'' | k'' \rangle. \tag{60}$$

The matrix element formed by the combination of a linear momentum bar and a position ket vector is given by

$$\langle r | k \rangle = \frac{1}{(2\pi)^{3/2}} \mathrm{e}^{-\mathrm{i}k\cdot r}. \tag{61}$$

Inserting (56), (60) and (61) into (59) and making use of the "delta function" in the form

$$\delta(k) = \frac{1}{(2\pi)^3} \int \mathrm{d}r \mathrm{e}^{\mathrm{i}k\cdot r}, \tag{62}$$

the magnetic structure factor takes the form

$$F_M^S(k) = -\mu_\mathrm{B} \int \mathrm{d}k S(k) u^*(k') u(k - k') n. \tag{63}$$

In explicit form and including the spin up and spin down notation of $u(k)$ the above equation may be written as

$$F_M^S(k) = -\mu_\mathrm{B} \int \mathrm{d}k' \left[\left(u^\uparrow(k')\right)^* u^\uparrow(k - k') - \left(u^\downarrow(k')\right)^* u^\downarrow(k - k') \right] n. \tag{64}$$

Equations (63) and (64) are convolution integrals and nothing else but the Fourier transforms of (57) and (58). The magnetic structure factor as given in (64) is still generally valid and not yet restricted to the case of free electrons.

The integration in (64) becomes particularly simple for the case of free electrons. Their wave function is given by plane waves with $u(k)$ equal to a constant. The constant equals one for all occupied states, while the function $u(k)$ is equal to zero for k states which are not occupied. The energy dispersion for free electrons is given by a parabola with degenerate energy bands for spin up and spin down electrons.

In order to have a nonzero magnetic structure factor and a net ferromagnetic moment the energy bands for spin up and spin down electrons must be displaced in energy. This is illustrated in Fig. 2. The lifting of the degeneracy may be either due to an external magnetic field or due to an intrinsic ferromagnetic instability of the conduction electron band. The Fermi surface is assumed to be a sphere for both spin up and spin down electrons with the Fermi wave vectors given by $k_\mathrm{F}^\uparrow$ and $k_\mathrm{F}^\downarrow$, respectively.

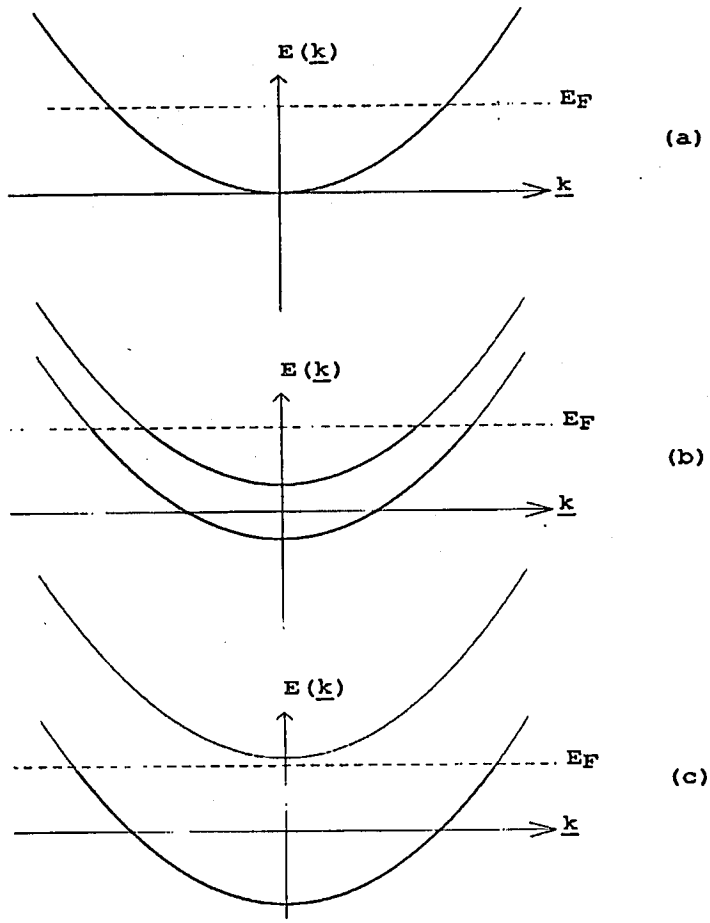

Fig. 2. Part (a) shows the band structure of free electrons without an applied magnetic field. The band is degenerate with respect to the spin orientation of the electrons. A magnetic field lifts this degeneracy and splits the bands into minority and majority bands. This yields a net polarization of the conduction electrons which, depending on the strength of the magnetic field, may result in a partial (part (b)) or a complete polarization (part (c)). The Fermi level E_F adjusts itself so as to ensure a constant number of conduction electrons.

The function $u^{\uparrow}(k-k')$ ($u^{\downarrow}(k-k')$) has a nonzero value ($\equiv 1$) in a sphere of radius $k_F^{\uparrow}$ ($k_F^{\downarrow}$). The centre of the sphere is located at k. Thus the convolution integral (64) reduces to the integration of the intersection of two spheres of equal radii and with their centres a distance $|k|$ apart. This situation is illustrated in Fig. 3. Using these geometric arguments and denoting $|k|$ by k the integral is

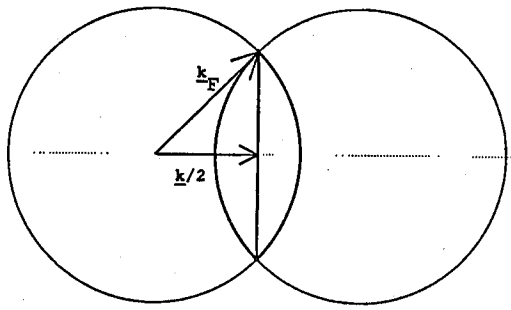

Fig. 3. Integration contour of Eq. (64). Two spheres with equal radii and with their centres placed a distance $|k|$ apart intersect each other over the region outlined by the thicker line. The three-dimensional picture is obtained by an out of the plane rotation of the above figure around the dotted line.

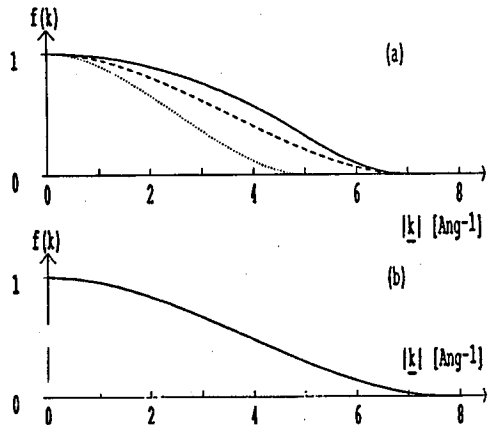

Fig. 4. Plot of the magnetic form factor for conduction electrons with a band structure as shown in Fig. 2b and 2c for parts (a) and (b), respectively. Part (a) shows the magnetic form factor of the minority band (dotted line), majority band (dashed line) and the total magnetic form factor (full line). Note that each form factor has been normalised to one at zero scattering vector. The magnetic form factor is zero for k values with $|k| \geq 2k_{\mathrm{F}}$. A conversion to a $\sin\Theta/\lambda$ scale on the x-axis is achieved by dividing by 4π the scale shown in the above figures.

evaluated to

$$\int \mathrm{d}k' \left(u^{\uparrow}(k')\right)^* u^{\uparrow}(k-k') = \begin{cases} \frac{\pi}{12}(2k_{\mathrm{F}}^{\uparrow} - k)^2(k_{\mathrm{F}}^{\uparrow} + k) & \text{for } k < 2k_{\mathrm{F}}^{\uparrow}, \\ 0 & \text{for } k \geq k_{\mathrm{F}}^{\uparrow}. \end{cases} \quad (65)$$

The spin down integral can be evaluated in an identical manner, and the magnetic structure factor is obtained by the subtraction of the results of the integration for spin up and spin down electrons.

The magnetic structure factor may be calculated for the two cases of complete and partial magnetic polarization of the electrons as illustrated in Fig. 2. The resulting magnetic structure factors are illustrated in Fig. 4, where the scattering vector dependence is plotted for the magnetic structure factor normalised to one at zero scattering vector by dividing $F_M^S(k)$ by the total magnetic moment.

The results of the integration in (64) shows that the contribution of the free electron magnetization to the magnetic structure factor is limited to low scattering vectors. An upper limit of the contribution may be obtained from (64) by considering the fully polarised state. For scattering vectors k with $k > \max(k_F^{\uparrow}, k_F^{\downarrow})$ the magnetic structure factor is zero for free electrons. A typical value for the Fermi wave vector may be chosen to be 2 Å. This results in an estimate of $1/\pi$ for the upper cut-off in $\sin\theta/\lambda$ for a free electron contribution. For a partially polarised state the upper cut-off will be reduced appropriately.

The magnetic structure factor for free electrons may be used to estimate the contribution of conduction electrons. While conduction electrons in real solids are delocalised they may not be entirely free (that is have a $u(k)$ as given above). But the free electron picture may serve as a reasonable guide to estimate their contribution to the magnetic structure factor.

In "real" solids, and taking rare earth alloys as an example, the main part of the magnetization is carried by localised magnetic moments which originate from $4f$-electrons. A polarization of the conduction electrons will give rise to a small additional magnetic moment, which will change the value of the total magnetic moment in the unit cell and influence the first few Bragg reflections. The total f-electron moment obtained by an extrapolation of the magnetic form factors or magnetic structure factors of higher scattering vectors to lower k values does not always agree with the total magnetic moment as obtained by magnetization measurements. The difference is usually attributed to a conduction electron polarization. As their contribution is confined to low scattering vectors it is sometimes approximated by a "delta function". There are only few Bragg reflections within the range of a nonzero free electron magnetic structure factor. Thus the detailed form of the magnetic structure factor is not readily investigated experimentally by using the technique discussed here. It is only due to a deviation of a few magnetic structure factors from their extrapolated values at low absolute scattering vectors (and most significantly at $k = 0$) that the conduction electron polarization may be detected. An approximation by some well localised and narrow function centred at zero scattering vector seems to be adequate to achieve consistency with observation.

It is a general feature of the Fourier transform that a localised contribution in one space will result in a Fourier transform which has a delocalised character. The inverse is also correct. As for the case of free electrons their wave function is delocalised in real space, thus giving rise to a sharply peaked magnetic structure factor. In order to have a magnetic structure factor which is more extended in reciprocal space the source of magnetization density must be more localised in real space.

The other extreme compared to the completely delocalised and free electrons

is given by completely localised electrons. Such cases are realized in rare earth and actinide metals and their alloys. The f-electron wave functions are well localised within the electron cloud of the free atom with a radius of the f-electron wave function which is much smaller than the radii of the outer s or p electrons. Thus, if atoms with a partially filled f-electron shell are alloyed into a solid, their f-electron wave functions do not overlap and they remain to a large degree atomic-like. However, complications arise due to an interaction with conduction electrons, resulting in a rich spectrum of physical properties including intermediate valency and heavy fermion behaviour.

For the purpose of analysing magnetic form factor measurements, however, the most important feature is the localization of those electrons which give rise to the magnetization in the unit cell. With the example of f-electron systems in mind it is to be expected that the magnetization of f-electrons can be uniquely and unambiguously assigned to a certain atom. The overlap integral is small between f-electron wave functions located on neighbouring atoms and the integral may be approximated by zero for the purpose of calculating the magnetization density. It suffices to consider only the localised contributions to the magnetization density with a wave function $|\Psi\rangle$ for the whole crystal given in a tight binding approximation. For simplicity it is assumed that only one atom per unit cell is contributing to the localised magnetization density. Within a band picture the f-electrons will give rise to a narrow band. This f-electron band will be characterised by only a very modest dispersion due to the smallness of the wave function overlap between f-electron atoms on neighbouring lattice sites. For real solids the dispersion of the f-electron band is mainly due to the hybridization with conduction electrons. In order to simplify the description, only one band will be considered.

The wave function $|\Psi\rangle$ has to take due account of the localization and at the same time also of the requirement of the Bloch theorem for wave functions in a periodic lattice. For a localised moment system in a tight binding approximation the state vector of the whole crystal may be expanded as

$$|\Psi\rangle = \int \mathrm{d}k\, a_k |\Psi_n(k)\rangle \tag{66}$$

using the complete and orthonormal basis set of Bloch state vectors $|\Psi_n(k)\rangle$. As pointed out above, only one band will be considered as a consequence of which the band index n will be fixed.

The transformation of a Bloch state vector to a vector in position space representation is given by

$$|\Psi_n(k)\rangle = \int \mathrm{d}r |r\rangle\langle r|\Psi_n(k)\rangle = \int \mathrm{d}r |r\rangle u_n(k,r) \mathrm{e}^{-\mathrm{i}k\cdot r}. \tag{67}$$

$u_n(k,r)$ is a periodic function with the periodicity of the lattice. For the case of one magnetic atom per unit cell and within a tight binding approximation the function $u_n(k,r)$ takes the form

$$u_n(k,r) = \frac{1}{\sqrt{N}} \sum_i \mathrm{e}^{-\mathrm{i}k\cdot R_i} \Phi(r - R_i). \tag{68}$$

The function $\Phi(r-R_i)$ is a wave function which is assumed to describe the localised contribution arising from the i-th atom located at R_i. R_i is a lattice vector of the

crystallographic lattice. The number N is equal to the number of unit cells in the crystal which, for the conditions specified above, is equivalent to the number of magnetic atoms in the crystal. The overlap is assumed negligible with

$$\int \mathrm{d}r \Phi^*(r - R_i)\Phi(r - R_j) \approx 0 \quad \text{for} \quad i \neq j. \tag{69}$$

It is often assumed that $\Phi(r)$ is given in terms of wave functions which are characteristic of the free atom. It may be composed of several parts according to

$$\Phi(r - R_i) = \sum_\alpha a_\alpha \eta_\alpha(r - R_i) \tag{70}$$

with all functions $\eta_\alpha(r)$ of the expansion being located at the position of the i-th atom. This allows the lifting of degeneracy of an atom in a crystalline environment as compared to a free atom to be taken into account. For $4f$-electron systems the reduction in symmetry lifts the degeneracy of the $4f$ levels. The $4f$ energy levels split into crystalline electric field levels with the degeneracies of the levels being determined by the point symmetry of the atomic position. Here, however, the splitting of the f-electron band or f-electron levels will not be considered further.

The matrix element for the magnetization density in real space is given by

$$M(r) = \langle \Psi | \widehat{M}(r) | \Psi \rangle = \int \mathrm{d}k' \int \mathrm{d}k'' \int \mathrm{d}r' \int \mathrm{d}r'' \langle \Psi | \Psi_n(k') \rangle \langle \Psi_n(k') | r' \rangle$$
$$\times \langle r' | \widehat{M}(r) | r'' \rangle \langle r'' | \Psi_n(k'') \rangle \langle \Psi_n(k'') | \Psi \rangle. \tag{71}$$

In (71) the magnetization operator includes the spin and orbital contribution. With the state vector as specified above in (66) the matrix element for the magnetization takes the form

$$M(r) = \int \mathrm{d}k' \int \mathrm{d}k'' \int \mathrm{d}r' \int \mathrm{d}r'' a_n^*(k') a_n(k'') u_n^*(k', r')$$
$$\times M u_n(k'', r'') \mathrm{e}^{\mathrm{i}k' \cdot r'} \mathrm{e}^{-\mathrm{i}k'' \cdot r''} \delta(r' - r'') \delta(r - r'')$$
$$= \int \mathrm{d}k' \int \mathrm{d}k'' a_n^*(k') a_n(k'') u_n^*(k', r') M u_n(k'', r'') \mathrm{e}^{\mathrm{i}(k' - k'') \cdot r}. \tag{72}$$

Inserting the matrix element $u_n(k, r)$ in (68) into the above formula, $M(r)$ takes the form

$$M(r) = \frac{1}{N} \int \mathrm{d}k' \int \mathrm{d}k'' a_n^*(k') a_n(k'')$$
$$\times \sum_{i,j} \Phi^*(r - R_i) M \Phi^*(r - R_j) \mathrm{e}^{\mathrm{i}k' \cdot R_i} \mathrm{e}^{-\mathrm{i}k'' \cdot R_j} \mathrm{e}^{-\mathrm{i}(k' - k'') \cdot R_i}. \tag{73}$$

Because of the assumption of negligible overlap between neighbouring lattice sites the summation over the index j will only give a contribution for the term $i = j$. Thus (73) may be written as

$$M(r) = \frac{1}{N} \int \mathrm{d}k' \int \mathrm{d}k'' a_n^*(k') a_n(k'')$$
$$\times \sum_i \Phi^*(r - R_i) M \Phi^*(r - R_j) \mathrm{e}^{\mathrm{i}(k' - k'') \cdot R_i} \mathrm{e}^{-\mathrm{i}(k' - k'') \cdot r}. \tag{74}$$

With a shift of the origin by R_i (i.e. by a variable transformation $r - R_i \rightarrow r$) and with the help of the "delta function"

$$\delta(k - k') = \frac{1}{N} \sum_i e^{i(k-k')\cdot R_i} \tag{75}$$

the magnetization density in real space is finally obtained as

$$M(r) = \int dk |a_n(k)|^2 \Phi^*(r) M \Phi(r). \tag{76}$$

The factor $\int dk |a_n(k)|^2$ is nothing else but an occupation factor, which in real space corresponds to an average occupation of the level, or levels, included in $\Phi(r)$. The remaining factor $\Phi^*(r) M \Phi(r)$ yields the magnetization density in terms of the wave function which describes the localised contribution. The occupation factor may be absorbed into $\Phi(r)$, which then corresponds to a wave function composed of a sum over all occupied states with weighing factors according to the occupation of the various levels.

As pointed out above a frequently used approximation is to take the functions $\Phi(r)$ to be given by those of a free atom. This is the reason why free atom form factors are so often employed for an explanation of magnetization density measurements. It is worth recalling the definition of the magnetic form factor $f(k)$ as given in (15) where $f(k)$ was defined as the Fourier transform of the magnetization density of a single atom. The results of calculations of atomic magnetic form factors for rare earth and actinide atoms have been tabulated in the literature both, for nonrelativistic [13] and relativistic [14] calculations.

Thus, the calculation of the magnetization density in real space has been reduced to the calculation of the magnetization density of a free atom. Both spin and orbital contributions to the magnetization are more readily calculated for the free atom compared to a determination by a band structure calculation. Other interactions such as spin–orbit coupling and crystal field interactions with the crystalline environment may also be included. Particularly for the interactions which give rise to the crystalline electric fields it is an advantage that for localised and atomic-like wave functions it is possible to separate the wave function into an angular and a radial part.

By transforming to spherical coordinates the wave function $\Phi(r)$ may be written in the form $\Phi(r) = R(r)\, Y(\vartheta, \varphi)$. The angular part of the wave function is readily treated thoroughly taking into account the removal of spherical symmetry and the lifting of degeneracies in the crystal. Group theory predicts the splitting and the level degeneracies. The remaining matrix elements which are not fixed by symmetry considerations are commonly taken as free parameters to be fixed by comparison with experiments.

A complete derivation of the mathematics is given in [15, 16] and in Lovesey [2]. The case of crystal fields has been considered by Boucherle [17]. The radial part of the wave function is not determined by symmetry alone but it is a rather complicated function of r. Its full and satisfactory determination requires a full scale relativistic calculation for the free atom. To go beyond this approximation necessitates a full scale band structure calculation. This, however, is often not feasible and the radial dependence of a free atom calculation is used for comparison with experiment.

The problem of calculating the magnetization density in the unit cell has thus been reduced to the calculation of the magnetization of a single atom. Under the assumption that it is adequate to treat the atom in the crystal essentially in the same manner as a free atom all the standard procedures of spectroscopy may be applied. While the mathematical procedure may be involved it is nevertheless straightforward. A complete exposition of the physics of spectroscopy is given in the book by Condon and Odabasi [18], and it should be consulted in addition to the references cited above.

After the discussion of the calculation of the magnetization density in real space an experimental investigation will be considered in the next section. Experimental results are presented and the magnetization densities are interpreted and discussed in relation to the models of localised and itinerant electron magnetization densities.

4. Experimental investigation

The investigation of the magnetic form factor and the magnetization densities in a solid commences with a proper characterization of the nuclear structure. Therefore, the first part of this section will be concerned with the determination of the nuclear structure as defined by the identification of the atomic positions. In the second part data will be presented of the magnetic form factor and magnetization density, and an interpretation will be given of the observation.

Two substances will be considered here, UBe_{13} and UPt_3, with both compounds belonging to the group of heavy fermion superconductors. The properties of heavy fermion systems are of interest in themselves, and their investigation is currently a very active field of research. However, the physical properties of heavy fermions are not of primary interest here, but rather attention is focused on their magnetic form factors only. Therefore, out of the rich spectrum of heavy fermion properties it is only the static magnetic characteristics as seen in an investigation of the magnetization densities which are of interest here.

4.1. Nuclear structure of UBe_{13} and UPt_3

The crystallographic structure of UBe_{13} and UPt_3 is cubic and hexagonal, respectively. The crystallographic space groups proposed in the literature [19] are given as $Fm\bar{3}m$ for UBe_{13} and $P6_3/mmc$ for UPt_3. These structures have been confirmed in a detailed neutron scattering experiment, and the free parameters have been determined experimentally for these structures as given by the positional parameters of one Be atom position in UBe_{13} and the position of the Pt atom in the unit cell of UPt_3. Additional information was obtained in these experiments with regard to temperature factors, absorption and extinction.

The nuclear structure of UBe_{13} is presented in Fig. 5 as a projection of the atomic positions onto one of the cubic faces. Each unit cell contains 8 formula units, with 8 U atoms and 104 Be atoms on two crystallographically different positions. Denoting the two Be sites by BeI and BeII, there are 8 BeI and 96 BeII atoms shown in the projection. For clarity a projection is shown in Fig. 5b which contains

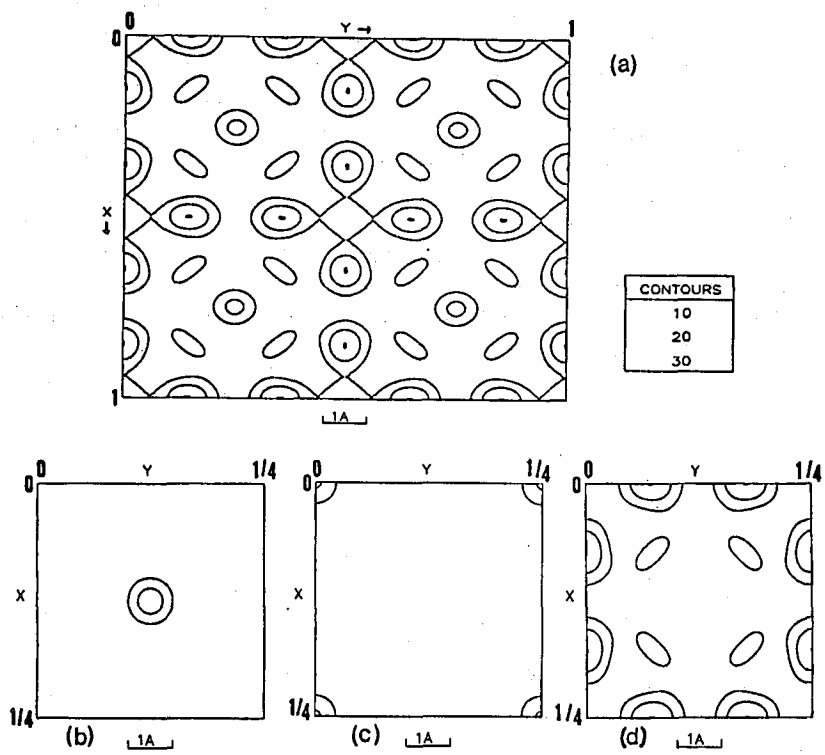

Fig. 5. Projection of the nuclear structure of UBe_{13} onto one of the faces of the cube. There are 8 formula units within a unit cell and the projected positions of all 112 atoms are shown in part (a). Parts (b) to (d) show only 1/4 of the projected unit cell with the positions of U atoms (part (b) with two U atoms being projected down onto the cube's face) and the two Be atom positions in parts (c) and (d) with 8 and 96 atoms per unit cell, respectively.

only the U atom positions. The uranium and BeI atoms each form a simple cubic sublattice within the UBe_{13} structure. For the projections shown in Fig. 5b there are two U atoms being projected down onto each uranium site.

It is worth pointing out some of the features of the projection of the nuclear density in Fig. 5. First of all, it is a map in real space of the neutron–nuclei interaction potential. It is obtained by a Fourier transformation using the nuclear structure factors in a manner identical to the procedures described above for the magnetization density. The nuclear density is seen to be smeared out over a small region with the centre of the density being located at the position of the atom. This smearing is a consequence of the finite Fourier series which has been used to obtain the nuclear density. The "real" interaction potential is a "delta function" when a standard description of the interaction potential is used with the Fermi approximation. Thus, the finite width in the nuclear density map is entirely due

to the number of the Fourier coefficients used in the Fourier inversion. In order to allow a comparison with the magnetization density map the same cut-off is used in the Fourier series as will be used later in the construction of the magnetization density. In studying the projection of the nuclear density it should also be taken into account that the nuclear density is measured by the strength of the neutron– nucleus interaction. The strength of the interaction potential is parameterized by the neutron scattering lengths b_U and b_{Be} [20]. However, due to very similar values of the scattering lengths for U and Be ($b_U = 8.41 \times 10^{-15}$ m, $b_{Be} = 7.79 \times 10^{-15}$ m) it is difficult to distinguish the U and Be atom positions from the values of the contour levels in Fig. 5.

For UPt_3 the nuclear structure is shown in Fig. 6 as a three-dimensional picture. Figure 7 shows the position of the U and Pt atom for two cuts through

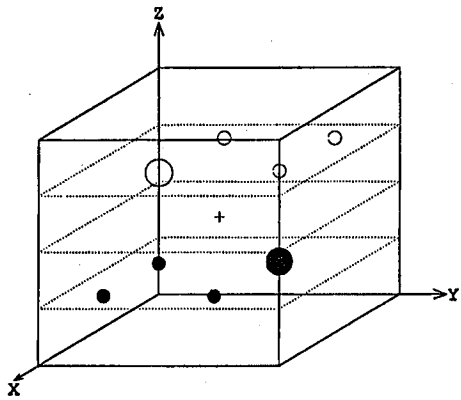

Fig. 6. Hexagonal unit cell of UPt_3. There are two formula units within a unit cell arranged on two planes with $z = 1/4$ and $z = 3/4$. The origin of the unit cell and the point (1/2, 1/2, 1/2) are centres of inversion symmetry.

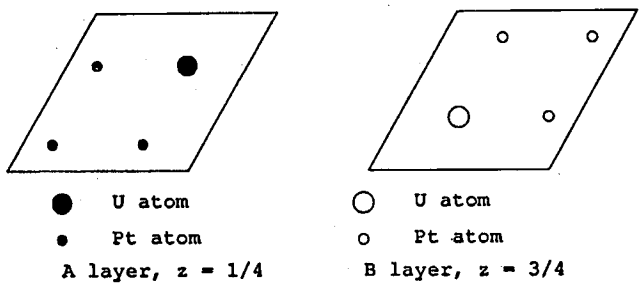

Fig. 7. Arrangement of U and Pt atoms in UPt_3 within the two hexagonal planes at $z = 1/4$ and $z = 3/4$.

the unit cell. The unit cell of UPt_3 contains two formula units with the atoms located in two hexagonal planes with $z = 1/4$ and $z = 3/4$ and as shown in Fig. 7. Both planes are related to one another by centres of inversion symmetry which are located at the origin of the unit cell (0, 0, 0) and at the position (0.5, 0.5, 0.5).

Both nuclear structures are centrosymmetric as a consequence of which the nuclear structure factors can be chosen real. Therefore, the phase factor of the nuclear (and also of the (ferro-) magnetic) structure factor is given by either +1 or −1. Both materials are paramagnetic in the temperature range investigated in the form factor measurement. For UPt_3 antiferromagnetic order is reported to occur at approximately 5 K with a doubling of the unit cell. This, however, will not interfere with the form factor measurements and therefore the antiferromagnetic order of UPt_3 will not be pursued further.

4.2. Magnetic form factor measurements in UBe_{13} and UPt_3

In the spin polarised neutron scattering experiment the samples were placed in a magnetic field of 4.6 tesla. For the UBe_{13} sample the magnetic field direction was parallel to the crystallographic [1, 1, 0] direction, while for UPt_3 the magnetic field was along [2, 1, 0]. For UPt_3 this corresponds to a configuration where the field is in the hexagonal plane and perpendicular to the magnetically hard direction which is found to be given by the crystallographic c-axis.

The flipping ratios of a number of the Bragg reflections have been measured at temperatures of 10 K for UBe_{13} and for 5 K and 23 K for UPt_3. As the flipping ratios for UPt_3 did not vary with temperature, the two data sets were merged in order to improve statistics.

In the spin polarised neutron scattering experiments the flipping ratios have been obtained for all measurable Bragg reflections with values of the scattering vectors characterised by $\sin\Theta/\lambda < 0.5$ Å^{-1}. In order to present the data in a concise and meaningful manner one may assume that the magnetization arises only from the $5f$ electrons located on the uranium atom. Due to the simplicity of the structures for both UBe_{13} and UPt_3 it is possible to reduce the magnetic structure factor to the magnetic form factor of the uranium atom. Within this model of only taking into account the $5f$-electron magnetization and by using (14) and (15) the magnetic structure factor can be written as

$$F_M(\tau) = \sum_i \mu_i f_i(\tau) e^{i\tau \cdot r_i}. \tag{77}$$

Here the summation is carried out over all uranium atoms with their positions given by r_i within the unit cell. According to the assumption made above all other atoms in the unit cell do not contribute to the magnetization and therefore they need not be included in the summation in (77). Moreover, all uranium atoms are on crystallographically equivalent positions and their induced magnetic moments are all equal. Thus with

$$f_i(\tau) = f(\tau), \qquad \mu_i = \mu \tag{78}$$

the magnetic form factor reduces to

$$F_M(\tau) = \mu f(\tau) \sum_i e^{i\tau \cdot r_i}. \tag{79}$$

The factor $\sum_i e^{i\tau \cdot r_i}$ is a known entity as all the parameters such as atomic positions are known. Thus, this factor may readily be removed from (79). Thereby, the magnetic structure factor is reduced to the magnetic form factor of the uranium atom multiplied by a constant. The multiplicative factor in front of the magnetic form factor is equal to the total ferromagnetic moment located on the uranium atom.

The magnetic form factor of the uranium atom is the Fourier transform of the atomic magnetization density. These densities have been calculated for the various states of ionization of the free uranium atom, and the relevant functions have been tabulated in the literature [14]. Assuming that three $5f$-electrons are present on the uranium atom and that crystal field splittings and hybridization effects can be neglected, the magnetization density of the uranium atom retains its spherical symmetry within the crystalline environment. A magnetic form factor which is evaluated under these assumptions is known as a form factor in dipole approximation.

Using the dipole approximation for the $5f$-electron magnetization there remains only one free parameter to be determined by comparison with experiment. The unknown entity is given by the size of the magnetic moment located on the uranium atom. While the saturation magnetic moment of this configuration can be calculated, the magnetic moment aligned by the external magnetic field and at the relevant temperature may be substantially different from the total magnetic moment on the atom. Thus, with the assumption of a localised magnetization density centred on the Uranium atom and within a dipole approximation for the magnetization distribution a one-parameter fit has to be carried out.

The results of such a fitting procedure are shown in Fig. 8 and Fig. 9. The continuous line corresponds to the magnetic form factor of the uranium atom while the data points are given by the measurements on UBe_{13} and UPt_3. While the experimental values of the magnetic form factor of UBe_{13} are satisfactorily reproduced by a form factor of the Uranium atom in dipole approximation, the corresponding data points for UPt_3 show a significant scatter around the curve of a spherically symmetric magnetization distribution.

In order to improve the agreement between calculation and observation for UPt_3 one may try to relax the condition of a spherically symmetric magnetization distribution and model the form factor within a crystal field model. However, even within this less stringent model the agreement of an improved model calculation and experimental observation is poor. It turns out that the scatter of the data points in Fig. 9 is too varied to allow modelling using only an uranium atom magnetization.

In order to obtain more insight into the reason for such a discrepancy and to be able to identify the various contributions to the magnetization it is informative to study the magnetization density in real space. Using the measured magnetic structure factors in the Fourier series, the real space magnetization densities have been constructed for both, UBe_{13} and UPt_3.

The magnetization density in UBe_{13} is shown in Fig. 10 as a projection onto one of the faces of the cubic unit cell. The number of the Fourier coefficients and the other conditions for obtaining the plot are the same as the one for the projection

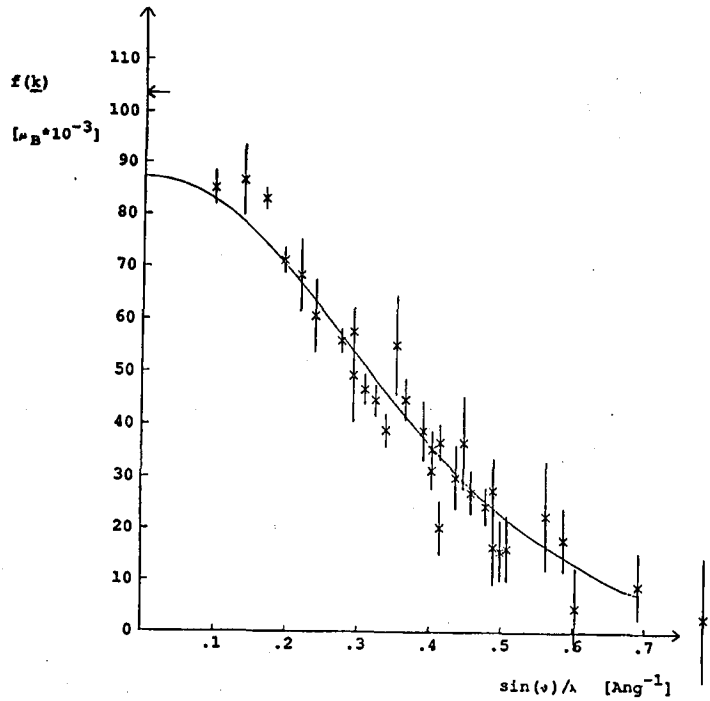

Fig. 8. Magnetic form factor of UBe_{13} as deduced from measurement (crosses) and as calculated (line) using a spherically symmetric free-atom-like magnetization distribution centred on the uranium atom. The theoretical calculation is obtained by a one-parameter fit to the experimental data assuming a f^3 configuration of the uranium atom. For details see text.

of the nuclear density in Fig. 5. It is seen from the magnetization projection that a magnetic density arises at the positions of the uranium atoms. No other structure or detail is visible within the unit cell. In particular, there is no localised magnetic contribution centred at the Be atom positions.

This result is not surprising in view of the fact that the magnetic form factor fit in Fig. 8 is a good description of the experimental data. The magnetization density in real space is therefore dominated by the $5f$-electron magnetization. However, for low scattering vectors a systematic deviation is found in Fig. 8 between the observed data points and the calculated form factor curve. This deviation at low values of $\sin\theta/\lambda$ is attributed to a polarization of the conduction electrons. As discussed in some detail in Sec. 3, the conduction electron contribution will be sharply peaked at $\tau = 0$ and quickly fall to zero as the size of the scattering vector increases. The Fourier transform is not expected to show significant structure.

In order to illustrate the effects of an incomplete Fourier series a magnetization density map is constructed with one component missing. Such a picture is shown in Fig. 11, where the component corresponding to $\tau = (2, 2, 0)$ has been

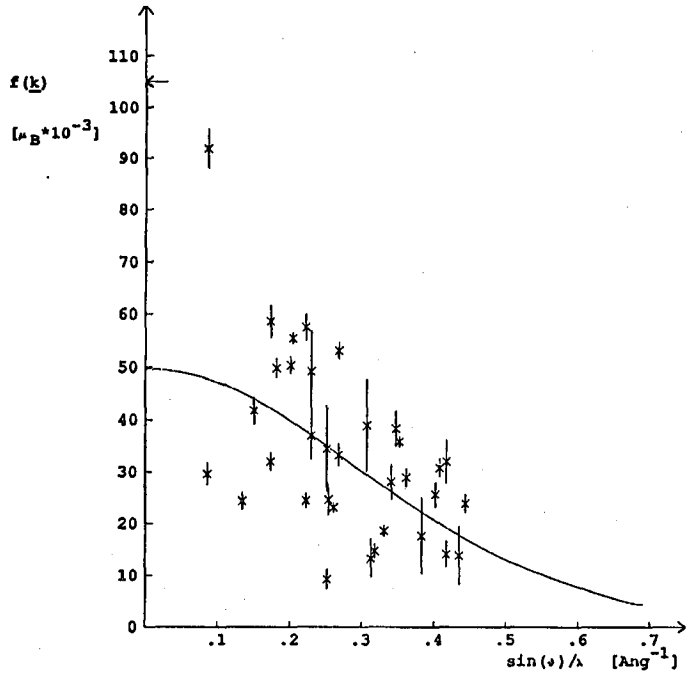

Fig. 9. Experimental (crosses) and theoretical (line) magnetic form factor for UPt_3. The magnetic form factor calculation was carried out in the dipole approximation. This model assumes that the magnetization is carried exclusively by uranium $5f$-electrons with the calculation being carried out for a spherically symmetric magnetization distribution. As seen from this picture this model is a very poor representation of the data. More refined models which lift the restrictions of spherical symmetry but keep an "uranium atom only magnetization contribution" do not differ appreciably from the simple calculation presented here. The experimental data is too varied to be explained by an anisotropic magnetization distribution. For details see text.

reduced by a factor of two. The nuclear structure factor of this reflection is accidentally very small, as a consequence of which it is experimentally more involved to obtain accurate values of the flipping ratio. This is due to experimental difficulties and uncertainties which arise in an accurate determination of the background contribution for weak reflections. For reflections with a low nuclear structure factor other contributions such as those due to multiple scattering may seriously influence the intensity of the Bragg reflection. Thus, the flipping ratio of a weak reflection may be systematically estimated as being either too low or too high. For a magnetization density map which is constructed using this coefficient in the Fourier series the resulting magnetization density may show additional structure which arises from the difference between the correct and estimated magnetic structure factor. Figure 11 shows magnetization density for the magnetic structure factor

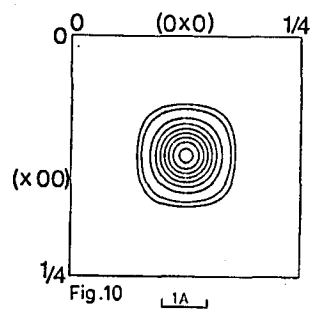

Fig. 10. Projection of the magnetization density in real space for UBe_{13} as obtained by the Fourier transformation from the experimental data (see also Fig. 8). For clarity only 1/4 of the unit cell is shown. The projection corresponds to the projection of the nuclear uranium atom positions as shown in Fig. 5b. The density has been averaged over a cube of edge 1 Å with the magnetic density levels corresponding to 5, 10, 30, 50, 70, 90, 110, 130 and 150 in units of 10^{-3} $\mu_B/Å^2$.

Fig. 11. Projection of the magnetization density in UBe_{13} onto one of the cubic faces. This figure corresponds to Fig. 10, with the difference that the contribution of the (2, 2, 0) reflection has been reduced by a factor of 0.5. The experimental determination of the flipping ratio of this reflection is particularly difficult due to an accidentally small nuclear structure factor (see text). The "additional features" in the magnetization density map are artefacts which are characteristic of a "missing component" in the Fourier series.

with the "correct" coefficient of the (2, 2, 0) reflection being multiplied by 0.5. This reflection and the ones obtained from it by the application of the symmetry elements of the structure contribute a term proportional to $\cos\left(\frac{4\pi}{a}(r_x + r_y)\right)$ to the projection of the magnetization density.

In order to see whether or not such structure in the magnetization density is a "real" effect or whether it arises due to some missing or wrong Fourier components one may calculate the magnetization using a simple model such as the uranium $5f$-electron magnetization only and employing the dipole approximation. This model may then be used to construct the magnetization density in real space by a Fourier transformation and with the same coefficients in the Fourier transform as used in the experimental series. Such a density map should then show only localised magnetic contributions. Any deviation from this must be attributed to an effect of the Fourier series. Alternatively, one may study the difference map, which is obtained by Fourier transforming the difference of observed and calculated magnetic structure factors. Both procedures enable to identify the origin of the structure which is found in the magnetization density maps.

Figure 12 shows the magnetization density for UPt_3 as a cut through the unit cell at a height of $z = 1/4$. The positions of the atoms in this plane are indicated in Fig. 7. When studying the magnetization density of Fig. 12, the first impression

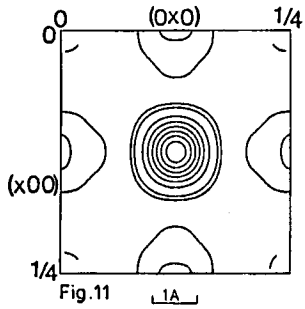

Fig. 12. Magnetization density in UPt_3. The picture shows a cut through the unit cell at $z = 1/4$. The atom positions in this plane are indicated in Fig. 7a. In addition to a $5f$-electron magnetization magnetic density can be attributed to uranium $6d$ and $7s$ electrons. The Pt atoms are seen to carry a significant magnetic moment. The platinum atom magnetization is delocalised and it does not resemble a density expected on the basis of free atom wave functions. The negative contour levels (dashed line) correspond to a magnetization density of -15, -10, -5 and -2.5, while positive levels (full lines) are given for the values 2.5, 5, 10, 20, 30, 40, 50, 60, 70 and 80 in units of 10^{-3} $\mu_B/Å^3$.

is one of a complex magnetization distribution with various contributions which are located at different positions in the unit cell.

Around the position of the uranium atom there is indeed a significant and well localised magnetization to be found. The radial extent of the $5f$-electron wave functions is consistent with the innermost magnetization distribution. However, in addition to the magnetization of the $5f$-electrons a magnetization contribution is identified which arises from $6d$ and $7s$ electrons of the uranium atom. The symmetry of the $6d$-electron wave functions is reduced due to the point symmetry of the uranium location. The threefold axis of rotation gives rise to the crystal field splitting of the $6d$-electron levels. This is the reason for finding the three regions of positive magnetization density at a distance of ≈ 1.2 Å of the U atom position. Both the radial extent of the wave function and the fact that it is split into crystal field levels uniquely identify this magnetization distribution as arising from $6d$ electron. For s or p electrons no splitting is expected to occur for the site symmetry of the uranium atom. The remaining negative magnetization distribution is attributed to a $7s$-electron polarization, with the $7s$-electron spin being orientated antiparallel to the direction of the $5f$-electron magnetic moment.

The remaining magnetization distribution in the unit cell arises due to a magnetic polarization of the platinum electrons. The Pt triangle within the unit cell is seen to carry a significant part of the magnetization density. The electrons have to be considered delocalised. The overlap between neighbouring Pt atom wave functions is significant, as a result of which the magnetization distribution is severely distorted. The appearance of the magnetization density does not any more resemble the one expected for atomic wave functions.

In order to model the magnetization density for UPt_3 all those electronic con-

tributions identified above have to be included. The model of a localised moment magnetization can be modified to include the localised magnetization contributions of the uranium atom. It suffices to use free atom wave functions. For the modelling of the magnetization density within the triangles of Pt atoms the overlap of wave functions has to be included. This requires a band structure calculation. Until now, however, a theoretical prediction of the magnetization density in UPt_3 based on the band structure calculation has not been reported in the literature.

Bearing these comments in mind a model calculation has been carried out using free atom wave functions for both, uranium and platinum contributions. By using such a model the agreement with observation could be significantly improved. The agreement is considered fair, however, with the main shortcoming of such a calculation being given by the inability to adequately model the delocalised magnetization density around the Pt atoms.

5. Discussion

The results of the form factor measurement of UPt_3 illustrate quite nicely the power of the technique of spin polarised neutron scattering. The magnetization density as presented in Fig. 12 reveals details of the electronic wave functions, their radial extent and the angular dependence. It is therefore a decisive test for any band structure calculation, whether or not such details of the electronic wave function are reproduced by the calculation. It was pointed out in the introduction that this type of measurement probes the ground state of the system. The perturbation which is introduced by the application of a magnetic field is of the order of 10 K. This energy is much smaller than the energies involved in typical experiments in spectroscopy, or the accuracy of energy values obtained by a band structure calculation. For the purpose of comparing the magnetic form factor measurements with results of band structure calculations the ground state wave function may be used for the calculation of $M(r)$.

In general, band structure calculations are aimed at a determination of the eigenvalues of the Hamiltonian of the system. This results in the energy spectrum as given by the band structure and the electronic density of states. In order to obtain good estimates for the energy eigenvalues of the system it is generally not required to have the exact wave function which is an eigenstate of the Hamiltonian. A method due to Ritz is a well known procedure in quantum mechanics whereby a trial wave function with some free parameters is used in a variational procedure to obtain estimates of energies for the system under investigation. Quite different wave functions may lead to very similar estimates for the energies. It is not essential to have the correct electronic wave function for obtaining good estimates for the band structure.

However, for obtaining a complete solution of a quantum mechanical system the eigenfunctions have to be determined. In this respect a comparison of calculated wave functions with the results of magnetic form factor measurements can be helpful. Spin polarised neutron scattering experiments are capable of yielding very detailed information on the wave functions of some electrons in the system.

In addition to providing a challenge for band structure calculations the mag-

netization densities may yield qualitative information on the degree of localization of electrons in metals and on chemical bonding in ionic compounds. A large number of systems have by now been investigated with this technique. The interested reader is referred to a compilation of references for magnetic form factor measurements (Boucherle [21]), which contains a large number of systems with varied physical characteristics. The detailed interpretation of experimental results also depends to a large degree on the systems which are considered. Here only the example of a metallic system with localised and delocalised electron magnetization contributions has been considered. For a more detailed discussion the literature [22–26] may be consulted in addition to the text books on neutron scattering [1–3].

6. Conclusions

An introduction has been given to the technique of spin polarised neutron scattering with an application to magnetic form factor measurements. Some experimental questions have been discussed. For the interpretation of the magnetization density two models have been considered: a localised moment system and a delocalised electron system with the electron described by free electron wave functions. The various points raised in these discussions have been illustrated with the experimental investigation of the heavy fermion systems UBe_{13} and UPt_3. These systems exhibit the full spectrum of electronic magnetization distributions in metals. For electrons with localised characteristics it includes contributions from $5f$-electrons of the uranium atom with the magnetization having spherical symmetry, crystal field split contributions of $6d$-electrons and $7s$-electron magnetization with no angular dependence. Delocalised electron contributions are found in magnetization density in real space.

The experimental technique of magnetic form factor measurements by neutron scattering is a powerful tool, which may yield detailed information concerning electronic wave functions. This information is complementary to other experimental techniques which investigate the energy spectrum and band structure of the solid. Magnetic form factor measurements are also a challenge to theory and band structure calculations. A closer comparison of the magnetization density in real space with electronic wave functions obtained in band structure calculation is highly desirable.

References

[1] G.L. Squires, *Introduction to the Theory of Thermal Neutron Scattering*, Cambridge University Press, Cambridge 1978.

[2] S.W. Lovesey, *Theory of Neutron Scattering from Condensed Matter*, Clarendon Press, Oxford 1984.

[3] W.G. Williams, *Polarised Neutrons*, Clarendon Press, Oxford 1988.

[4] P.J. Brown, in: *Electron and Magnetization Densities in Molecules and Crystals*, Ed. P. Becker, Plenum Press, New York 1980, p. 255; P.J. Brown, J.B. Forsyth, *Br. J. Appl. Phys.* **15**, 1529 (1964).

[5] J.B. Forsyth, in Ref. [4], p. 323.

[6] P.J. Brown, J.C. Matthewman, *The Cambridge Crystallographic Subroutine Library (A collection of FORTRAN subroutines for the use in crystallography)*, Internal ILL Report, ILL, Grenoble 1990.

[7] R.M. Moon, *Int. J. Magn.* **1**, 219 (1971).

[8] P.J. Brown, *Physica B* **137**, 31 (1986).

[9] R. Nathans, H.A. Alperin, S.J. Pickart, P.J. Brown, *J. Appl. Phys.* **34**, 1182 (1963); H.A. Alperin, P.J. Brown, R. Nathans, S.J. Pickart, *Phys. Rev. Lett.* **8**, 237 (1962).

[10] B.N. Harmon, *J. Phys. (France)* C7, 177 (1982).

[11] K.H. Oh, B.N. Harmon, S.H. Liu, S.K. Sinha, *Phys. Rev. B* **14**, 1283 (1976).

[12] J.F. Cooke, S.H. Liu, A.J. Liu, *Phys. Rev. B* **37**, 289 (1988).

[13] M. Blume, A.J. Freeman, R.E. Watson, *J. Chem. Phys.* **37**, 1245 (1962).

[14] A.J. Freeman, J.P. Desclaux, *J. Magn. Magn. Mater.* **12**, 11 (1979); C. Stassis, H.W. Deckman, B.N. Harmon, J.P. Desclaux, A.J. Freeman, *Phys. Rev. B* **15**, 369 (1977).

[15] E. Balcar, *J. Phys. C, Solid State Phys.* 8, 1581 (1975).

[16] D.E. Rimmer, S.W. Lovesey, *Rep. Prog. Phys.* **32**, 333 (1969).

[17] J.X. Boucherle, D. Givord, J. Schweizer, *J. Phys. (France)* C7, 199 (1982).

[18] E.U. Condon, H. Odabasi, *Atomic Structure*, Cambridge University Press, Cambridge 1980.

[19] P. Villars, L.D. Calvert, *Pearson's Handbook of Crystallographic Data for Intermetallic Phases*, American Society of Metals, Witznau (Switzerland) 1985.

[20] V.F. Sears, *Thermal Neutron Scattering Lengths and Cross-Sections for Condensed Matter Research*, Chalk River Nuclear Lab., Chalk River (Canada) 1984.

[21] J.X. Boucherle, *A Compilation of Magnetic Form Factors and Magnetization Densities*, Neutron Diffraction Commission of the Internat. Union of Crystallography, ILL, Grenoble 1988.

[22] J. Schweizer, in Ref. [4], p. 501.

[23] J. Schweizer, in Ref. [4], p. 479.

[24] P.J. Brown, in Ref. [4], p. 723.

[25] J.B. Forsyth, in Ref. [4], p. 791.

[26] R.M. Moon, *J. Phys. (France)* C7, 187 (1982).